

ASD TECHNICAL REPORT 61-296

**STUDY OF THE EFFECT OF MELTING PRACTICE  
ON THE FATIGUE BEHAVIOR OF HIGH-STRENGTH STEEL**

**HARVEY B. NUDELMAN  
JOHN P. SHEEHAN**

**ARMOUR RESEARCH FOUNDATION  
OF ILLINOIS INSTITUTE OF TECHNOLOGY**

**NOVEMBER 1961**

**DIRECTORATE OF MATERIALS & PROCESSES  
CONTRACT No. AF 33(616)-6290  
PROJECT No. 7381  
TASK No. 73812**

**AERONAUTICAL SYSTEMS DIVISION  
AIR FORCE SYSTEMS COMMAND  
UNITED STATES AIR FORCE  
WRIGHT-PATTERSON AIR FORCE BASE, OHIO**

600 - January 1962 - 19-778 & 779

## FOREWORD

This report was prepared by Armour Research Foundation of Illinois Institute of Technology, Chicago, Illinois, under USAF Contract No. AF 33 (616)-6290. This contract was initiated under Project No. 7381, "Metallic Materials," Task No. 73812, "Behavior of Metals." The work was administered under the direction of the Directorate of Materials and Processes, Deputy for Technology, Aeronautical Systems Division, with Mr. K. D. Shimmin acting as project engineer.

This report covers work conducted from March 1960 to June 1961.

Personnel at Armour Research Foundation who contributed to the research program were R. Knight, H. Nudelman, and J. Sheehan. Data used in this report are recorded in Armour Research Foundation Logbooks C 1098, C 9785, and C 10613, assigned to ARF Project No. 2172. The report is designated internally as ARF 2172-22.

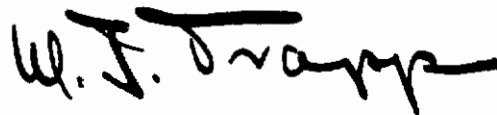
## ABSTRACT

Special carbon-aluminum deoxidation practice provided a significant increase in the fatigue properties of an induction-melted nickel-molybdenum high-strength steel. Prot evaluation of cylindrical R. R. Moore fatigue specimens gave  $E_p/UTS$  ratios of 0.500 and 0.555 at ultimate tensile strength levels of 274 and 200 ksi respectively. This represented a marked improvement as compared to standard melting techniques and commercial high-strength steels at similar strength levels. Vacuum arc and vacuum induction remelting of the specially deoxidized material reduced the fatigue strength to lower values than that characteristic of standard melting practice. The fatigue properties of vacuum-melted high-purity raw materials were inferior to those prepared by induction melting, but superior to the remelting approach. The harmful effect of silicon additions on the fatigue properties of these steels was related to the sequence in which they were made; the damage was minimized by adding the silicon after the completion of the aluminum killing treatment. Notched nickel-molybdenum steels were relatively unaffected by notching, and good fatigue strengths were obtained. The fatigue data did not appear to correlate with melting practice on the basis of inclusion content, and this was more evident for the notched investigation. Nickel-molybdenum steels were prepared by standard practice and special carbon-aluminum practice and tested in axial fatigue in the notched and unnotched conditions. The resultant scatter was too great to indicate any definite trends, however. A tungsten-molybdenum high-strength steel, studied previously was subjected to notched Prot testing, and a slight degree of notch sensitivity was found; two higher carbon versions of this steel were investigated for potential high-temperature spring applications by hot tensile and stress-rupture techniques.

## PUBLICATION REVIEW

This report has been reviewed and is approved.

FOR THE COMMANDER:



W. J. TRAPP  
Chief, Strength and Dynamics Branch  
Metals and Ceramics Laboratory  
Directorate of Materials and Processes

## TABLE OF CONTENTS

	PAGE
I. SCOPE . . . . .	1
II. INTRODUCTION . . . . .	2
III. EXPERIMENTAL PROCEDURE . . . . .	3
A. Steel Selection . . . . .	3
B. Melting . . . . .	3
C. Hot Working . . . . .	5
D. Machining and Heat Treatment . . . . .	6
E. Testing Procedure . . . . .	6
IV. RESULTS . . . . .	7
A. Chemical Composition . . . . .	7
B. Tensile Data . . . . .	7
C. Fatigue Data . . . . .	7
V. DISCUSSION . . . . .	7
VI. SUMMARY . . . . .	12
VII. CONCLUSIONS . . . . .	13
VIII. BIBLIOGRAPHY . . . . .	14
APPENDIX I - DETAILED PROT TESTING DATA . . . . .	39

## LIST OF ILLUSTRATIONS

FIGURE		PAGE
1	R. R. Moore Rotating Beam Fatigue Specimens . . . . .	28
2	Stress-Rupture Diagram for Steels S-6 and S-8 . . . . .	29
3	Summary of Fatigue Data . . . . .	30
4	The Effect of Tempering Temperature on the Fatigue Properties of Ni-Mo Steel . . . . .	31
5	Steel 1 at High Magnification. Air Melt, Standard Deoxidation . . . . .	32
6	Steel 2A at High Magnification. Air Melt, C-Al Deoxidation . . . . .	32
7	Steel 3 at High Magnification. Air Melt, C-Al Deoxidation with 0.30% Si Addition . . . . .	32
8	Steel 4 at High Magnification. Air Melt, C-Al Deoxidation with Si Addition after Al Killing . . . . .	32
9	Steel J at High Magnification. Vacuum Arc Remelting of Alloy 2A Type . . . . .	33
10	Steel H at High Magnification. Vacuum Induction Remelting of Alloy 2A Type . . . . .	33
11	Steel RVC at High Magnification. Vacuum Arc Melting of Pure Raw Materials . . . . .	33
12	Steel DU at High Magnification. Air Melt with Iron Oxide and Ferrosilicon Additions . . . . .	33
13	Steel DLOB at High Magnification. Air Melt, C-Al Deoxidation . . . . .	34
14	Steel 1, Air Melt, Standard Deoxidation . . . . .	35
15	Steel 2A, Air Melt, C-Al Deoxidation . . . . .	35
16	Steel 3, Air Melt, C-Al Deoxidation with 0.30% Si Addition . . . . .	35
17	Steel 4, Air Melt, C-Al Deoxidation with 0.03% Si Addition after Al Killing . . . . .	35
18	Steel J, Vacuum Arc Remelting of Alloy 2A Type . . . . .	36

## LIST OF ILLUSTRATIONS (Continued)

FIGURE		PAGE
19	Steel H, Vacuum Induction Remelting of Alloy 2A Type . . .	36
20	Steel RVC, Vacuum Arc Melting of Pure Raw Materials . . .	36
21	Steel DU, Air Melt with Iron Oxide and Ferrosilicon Additions . . . . .	36
22	Steel D10B, Air Melt, C-Al Deoxidation . . . . .	37
23	Steel D10 at High Magnification. Air Melt, C-Al Deoxidation . . . . .	38
24	Steel D10, Air Melt, C-Al Deoxidation . . . . .	38
25	Rotating Beam Prot Diagram. Alloy 1, 450°F Temper . . . . .	53
26	Rotating Beam Prot Diagram Alloy 2A, 450°F Temper . . . . .	54
27	Rotating Beam Prot Diagram Alloy 2A, 1000°F Temper. . . . .	55
28	Rotating Beam Prot Diagram Alloy 2B Notched, 475°F Temper . . . . .	56
29	Rotating Beam Prot Diagram Alloy 3, 450°F Temper. . . . .	57
30	Rotating Beam Prot Diagram Alloy 4, 500°F Temper . . . . .	58
31	Rotating Beam Prot Diagram Alloy J, 475°F Temper . . . . .	59
32	Rotating Beam Prot Diagram Alloy H, 500°F Temper . . . . .	60
33	Rotating Beam Prot Diagram Alloy RVC, 475°F Temper . . . . .	61
34	Rotating Beam Prot Diagram Alloy DU, 550° + 600°F Temper . . . . .	62
35	Rotating Beam Prot Diagram Alloy DU Notched, 550° + 600°F Temper . . . . .	63

LIST OF ILLUSTRATIONS (Continued)

FIGURE		PAGE
36	Rotating Beam Prot Diagram Alloy D10B Notched, 1050°F Temper . . . . .	64
37	Rotating Beam Prot Diagram Alloy D10B Notched, 1225°F Temper . . . . .	65

## LIST OF TABLES

TABLE		PAGE
I.	Composition of Experimental Steels . . . . .	15
II.	Preliminary Sheet Tensile Properties of Nickel-Molybdenum Steel . . . . .	16
III.	Fatigue Bar Tensile Data . . . . .	17
IV.	Room-Temperature Tensile Data for Steels S-6 and S-8 . . . . .	18
V.	Elevated Temperature Tensile Data for Steels S-6 and S-8 . . . . .	19
VI.	900°F Stress-Rupture Data for Steels S-6 and S-8 . . . . .	20
VII.	Summary of Fatigue Data . . . . .	21
VIII.	Notched Axial Fatigue Data . . . . .	22
IX.	Unnotched Axial Fatigue Data . . . . .	23
X.	Melting Practice Ranked by Fatigue Strength at Similar UTS Levels . . . . .	24
XI.	Notched Properties of Nickel-Molybdenum Steels . . . . .	25
XII.	Notched Properties of Tungsten-Molybdenum Steels . . . . .	26
XIII.	Standard Deviation of Prot Fracture Stress Data . . . . .	27
XIV.	Fatigue Data, Steel 1, 450°F Temper . . . . .	40
XV.	Fatigue Data, Steel 2A, 450°F Temper . . . . .	41
XVI.	Fatigue Data, Steel 2A, 1000°F Temper . . . . .	42
XVII.	Fatigue Data, Steel 2B Notched, 475°F Temper . . . . .	43
XVIII.	Fatigue Data, Steel 3, 450°F Temper . . . . .	44
XIX.	Fatigue Data, Steel 4, 500°F Temper . . . . .	45
XX.	Fatigue Data, Steel J, 475°F Temper . . . . .	46
XXI.	Fatigue Data, Steel H, 500°F Temper . . . . .	47
XXII.	Fatigue Data, Steel RVC, 475°F Temper . . . . .	48

## LIST OF TABLES (Continued)

TABLE		PAGE
XXIII.	Fatigue Data, Steel DU, 550° + 600°F Temper . . . . .	49
XXIV.	Fatigue Data, Steel DU Notched, 550° + 600°F Temper . . . . .	50
XXV.	Fatigue Data, Steel D10B Notched, 1050°F Temper . . . . .	51
XXVI.	Fatigue Data, Steel D10B Notched, 1225°F Temper . . . . .	52

*Contrails*

STUDY OF THE EFFECT OF MELTING PRACTICE  
ON THE FATIGUE BEHAVIOR OF HIGH-STRENGTH STEEL

I. SCOPE

Research involving the study and improvement of the fatigue properties of high-strength steel has been actively carried on since 1 December 1955, when this series of studies was initiated at the Armour Research Foundation. The original program, WADC Technical Report 58-289, was concerned with the effects of melting practice and inclusion content on the fatigue properties of AISI 4340 steel heat-treated to 260 to 280 ksi. It was demonstrated that melting high-strength steel under vacuum or protective atmosphere resulted in improved fatigue properties. However, the most promising development involved air-induction melted steel initially deoxidized with carbon additions, rather than silicon, and finally deoxidized with aluminum. This technique produced a steel having a Prot endurance limit to tensile strength ratio of 0.55 and a constant stress endurance limit of 148 ksi. Both of these values represented significant advances.

The second program in this series, WADC Technical Report 59-86, was concerned with improving fatigue strength by elevated temperature tempering. Microstress relief in the areas adjacent to inclusions was suggested as a possible mechanism for this effect. In order to investigate this phenomenon, it was first necessary to develop temper-resistant steels capable of providing ultimate tensile strengths of 280 to 300 ksi after tempering in the 1000° to 1300°F range. Several steels related to two basic compositions were prepared which appeared to offer the required characteristics. Hardness measurements were used to make the original evaluation, and promising steels were tested more thoroughly with respect to tensile properties. The result of this program was the development of two classes of steels, based on tungsten-molybdenum and molybdenum-chromium, capable of retaining high strength after elevated temperature tempering.

The third program, WADD Technical Report 60-120, represented the logical combination of the approaches carried out during the preceding projects. The first aspect of this research involved an investigation into the effect of high-temperature tempering on the fatigue properties of a temper-resistant high-strength steel, and a suitable tungsten-molybdenum steel was selected for this work. The second aspect was concerned with the application of special deoxidation techniques to temper-resistant steel. Several temper-resistant compositions were prepared in this manner as well as by standard induction melting practice. Fatigue tests of these steels clearly indicated that special deoxidation practice contributed to a very significant improvement in the Prot endurance limit. Under comparable conditions, this value was increased from approximately 100 to 141 ksi. A Prot endurance limit to

Manuscript released by the authors 30 June 1961 for publication as an ASD Technical Report.

tensile strength ratio of 0.6 was developed in this work at tensile strengths in the 230 to 250 ksi range. Melting practice appeared to play a much greater role in determining fatigue strength than tempering temperature. However, there was some additional indication that increasing tempering temperature contributed to increased fatigue strength; however, this cannot yet be stated as a definite conclusion.

In view of the extreme effect of melting practice, the present program was directed toward an investigation of a variety of techniques, including induction, vacuum-induction, and vacuum-arc melting. Extraneous variables were minimized through the utilization of a single series of alloy steels and treatments. This program will attempt to document the effect of melting and deoxidation practice and, consequently, that of the presence of nonmetallic inclusions on the fatigue properties of an ultra-high strength steel.

## II. INTRODUCTION

The primary objective of this program was to determine the effect of melting and deoxidation practice on the Prot endurance limit of a nickel-molybdenum high strength steel. A wide range of melting techniques was investigated to provide various inclusion distributions. Standard induction melting, special carbon-aluminum deoxidation, and consumable electrode vacuum arc remelting techniques were included. In previous work, silicon was not used as an alloying element. In this instance, in deference to its industrial importance silicon was added at different stages of induction melting operations. Chemical composition, processing, and heat treatment were held constant within the limits of practicality to study melting practice as a single independent parameter. Material evaluation was accomplished by R. R. Moore Prot fatigue testing in both notched and unnotched conditions. Axial fatigue techniques were also used to investigate this material. Standard melting practice and the special carbon-aluminum melting technique representing both notched and unnotched conditions were utilized in this work.

The effect of notching was not examined during previous work. Consequently, a carbon-aluminum deoxidized heat of 0.50 C, 2.00 W, 1.00 Mo, and 0.50 per cent V steel was prepared for Prot testing in the notched and unnotched conditions. This steel with higher carbon contents was evaluated for potential high-temperature spring applications with respect to hot tensile and stress-rupture properties.

### III. EXPERIMENTAL PROCEDURE

#### A. Alloy Selection

An alloy steel having the following composition was selected as the base material for investigating the effect of melting practice:

C	0.50
Ni	2.00
Mo	1.00
Mn	0.050

A simple composition was used to limit the number of variables while providing the required strength level (250 to 300 ksi tensile strength) and sufficient hardenability to harden throughout a 3/4 in. diameter cross section upon oil quenching. In two cases, silicon was added during different stages of melting; this was to examine its effect with respect to inclusion content rather than as an alloy addition. The original heats were melted without manganese, but hot shortness was indicated during forging. The manganese addition remedied this situation and was utilized thereafter.

One of the tungsten-molybdenum steels (designated D10) tested during the preceding program was evaluated with respect to notched Prot fatigue properties. The high ratio of Prot endurance limit to ultimate tensile strength (approximately 0.6) noted previously dictated its choice here. The nominal composition of this material is given below.

C	0.45
W	1.91
Mo	1.02
V	0.44
Mn	0.81

Two higher carbon modifications of this steel, in the 0.60 to 0.75 per cent carbon range, were selected for evaluation as elevated temperature spring materials.

#### B. Melting

The various melting techniques used during this program are listed below.

- (1) Induction air melting, standard deoxidation. (2 lb/ton Al)
- (2) Induction air melting, C-Al deoxidation.
- (3) Induction air melting, C-Al deoxidation with a 0.30 per cent Si addition before Al killing.
- (4) Induction air melting, C-Al deoxidation with a 0.30 per cent Si addition after Al killing.
- (5) Vacuum arc remelting of 2.
- (6) Vacuum induction remelting of 2.
- (7) Vacuum arc melting of high-purity raw materials.
- (8) Air melting, with iron oxide and ferrosilicon additions.

# Contrails

In item 1, the standard practice consisted of melting down Armco iron in a 400 lb induction furnace, adding the alloy elements, and completely deoxidizing with 2 lb of aluminum per ton of steel. All of the ingots melted in the induction furnace were poured into separable steel molds having a capacity of about 60 lb. A conventional refractory hot top was used in conjunction with an exothermic compound for all of this work.

The special carbon-aluminum deoxidized melts were prepared as follows. Armco iron was melted down in a 400 lb induction furnace and the oxygen content reduced with high-carbon cast iron (containing approximately 4 per cent carbon) at 3000° to 3200°F. The thermodynamic tendency for carbon to reduce the oxides in molten iron increases with increasing temperature; for this reason carbon deoxidation was carried out at high temperatures. After equilibrium deoxidation was obtained, sufficient high-carbon iron was added to increase the carbon content to the desired level. The melt temperature was lowered, and the alloy additions were made. To minimize the presence of silicate inclusions, no silicon was used. Final deoxidation was accomplished with 2 lb of aluminum per ton just prior to pouring.

The silicon techniques, items 3 and 4, illustrate two procedures for determining the effect of silicon. In No. 3, the silicon was added with the alloy additions, and since the bath had been only partially deoxidized (with carbon) it would be expected to provide silicates as well as silicon in solid solution. In No. 4 the silicon was added after completely deoxidizing the bath with aluminum in an attempt to obtain a silicon-bearing steel with a minimum of silicate inclusions. This was considered important, since silicon, in varying amounts, is an alloy constituent of a majority of the high-strength steel alloys.

In vacuum arc remelting, a carbon-aluminum deoxidized ingot was used as an electrode in the consumable arc vacuum melting technique. This ingot was processed twice, and typical melting conditions were as follows:

Current	3500 amps
Vacuum	3-150 microns

The maximum vacuum was obtained prior to melting, and full pumping capacity was continued during the entire sequence to maintain the "hardest" dynamic vacuum possible. A 4 in. crucible was used for melting, and ingots weighing 15 to 25 lb were produced. The high temperatures inherent in this process were expected to promote the reduction of nonmetallic oxides by carbon as described above. An additional advantage in this instance was the presence of a dynamic vacuum during melting to remove the gaseous carbon-oxygen reduction products.

A laboratory scale vacuum induction furnace was used to remelt the carbon-aluminum deoxidized ingots. This unit has a rather small capacity (15 to 20 lb), and the original ingot had to be cut into two pieces. The charges were melted, heated to a pouring temperature of 2800° to 3000°F, and poured while in the vacuum chamber. A sand hot top was utilized during solidification as this was the only type available for this ingot size. During this operation the vacuum ranged from 10 to 200 microns. This operation

was included primarily to effect degassing, as no significant degree of oxide reduction could be expected under these circumstances.

The raw material sources for vacuum arc melting (item No. 7) were as follows:

<u>Material</u>	<u>Source</u>	<u>Approximate Purity, per cent</u>
Electrolytic iron	Crane Co., Metals Division	99.92
Electrolytic manganese	Union Carbide Metal Co.	99.90
Nickel shot	International Nickel Co.	99.96
Molybdenum metal	Wah Chang Corporation	99.90

The electrolytic iron was carburized commercially to a carbon level of 0.80 to 0.90 per cent, after which it was crushed to 1/4 in. pieces and pickled in a 50 per cent HCl solution. This was mixed with the pure iron to adjust the carbon content. Nickel and manganese were added to the melt in the as-received form while molybdenum was used in the form of a 50 per cent iron-molybdenum master alloy. Nonconsumable melting was performed in a 4 in. crucible with a tungsten electrode under a protective atmosphere of argon gas. The resulting ingot was then used as an electrode for further processing, and two vacuum consumable arc remelting operations were carried out as described above.

Iron oxide and silicon dioxide were added during air induction melting (item No. 8) to attain a high concentration of silicate inclusions. After melting down Armco iron, the alloying elements except carbon--including, in this instance, 0.50 per cent silicon--were added; the melt was held at 3000° to 3200°F to increase the degree of oxidation. Following this, the melt temperature was lowered and the carbon-bearing iron was added. The operation was completed by applying standard deoxidation practice (2 lb aluminum per ton of steel), and the heat was poured in the usual manner.

Another set of materials was prepared for this program. This consisted of a 0.50 per cent carbon, tungsten-molybdenum steel for studying notched properties; two higher carbon steels having the same base composition were also made up for investigating elevated temperature tensile and stress-rupture properties. These steels were melted with the special carbon-aluminum deoxidation technique as described previously.

## C. Hot Working

The induction melted steels were hot forged from an ingot size of about 4 in. in diameter by 13 in. long to 3/4 to 1 in. rounds. The vacuum arc-melted steel was hot forged into 3/4 in. rods from 4 in. diameter by 8 to 14 in. long ingots. The vacuum induction melted ingots were tapered having a diameter range of 2 to 3 in. across an 8 in. length, and were also hot forged into 3/4 in. round stock. A forging temperature of 1800° to 2000°F was utilized for all forging operations.

## D. Machining and Heat Treatment

The fatigue bars were rough machined and, after heat treatment, finished by grinding and longitudinal polishing. Austenitizing operations were carried out in an Inconel muffle containing an argon atmosphere to prevent oxidation and decarburization. Hardening was obtained by oil quenching. All tempering operations were performed in air, followed by air cooling.

Cylindrical R. R. Moore fatigue bars, shown in Figure 1, were used for testing. Notched fatigue bars had a similar configuration except that the gage diameter was 0.250 in. A 60° notch (included angle) was used with a notch radius of 0.012 in.; the notched gage diameter was 0.200 in. Preliminary tensile data on nickel-molybdenum steel were determined with rolled sheet specimens. These samples were pin loaded and had a gage cross section of about 0.375 in. by 0.080 in.

A button-end cylindrical specimen type selected by ASD was used for axial fatigue testing. The over-all specimen length was 4 1/2 in. The minimum smooth cross-section diameter was 0.200 in. for the unnotched specimen, and 0.270 in. for the notched specimen. In the latter case a 60° notch having a 0.030 in. radius was used, and the cross-sectional diameter under the notch was 0.200 in. Standard techniques were used to prepare conventional round room temperature, hot tensile, and stress-rupture specimens from the high-carbon tungsten-molybdenum steels for elevated temperature studies.

## E. Testing Procedure

Fatigue testing was limited to the Prot method, in which the motor driving the specimen was also used to drive a variable gear train terminating in an accurately calibrated spring balance. The spring balance was directly connected to the specimen-loading system, and a rider showed the breaking load on the balance. It was possible to maintain very accurate and constant loading rates with this system. The Prot testing apparatus employed a motor running at 10,000 rpm. Prior to testing, the specimens were cleaned of oil by wiping with a soft tissue soaked in acetone. The eccentricity of selected specimens was checked in the housings, and readjustments in seating were made until the total eccentricity was less than 0.003 in. The starting stresses used for Prot testing were 42 ksi and 76 ksi for notched and unnotched fatigue specimens, respectively. The axial fatigue testing study was carried out at ASD using standard techniques.

Preliminary sheet tensile data on fatigue materials were obtained in the normal manner. Tensile data on the finished material were determined on randomly selected fatigue bars. This was done to establish meaningful values of the ultimate tensile strength; the yield strength could not be measured by this method, however.

Standard techniques were used to determine the room and elevated temperature tensile properties and the stress-rupture characteristics of two high-carbon tungsten-molybdenum steels.

#### IV. RESULTS

##### A. Chemical Composition

The analyses of the steel alloys studied in this program are shown in Table I. The melting practice used for each steel is indicated in the Table.

##### B. Tensile Data

Preliminary sheet tensile data on fatigue material steels are given in Table II. These results were included to indicate the yield strength level of this steel alloy series. Fatigue bar tensile data appear in Table III. The room temperature tensile, hot tensile, and stress-rupture data relating to the tungsten-molybdenum steels are given in Tables IV, V, and VI. The stress-rupture data are shown graphically in Figure 2.

##### C. Fatigue Data

The fatigue data are presented in complete form in Appendix I, Tables XIV through XXVI. A graphical summary of these results appears in Figure 3. The Prot endurance limits were determined by inserting the average failure stress and square root of the rate values into the two-point straight-line equation and solving for the failure stress at zero rate. Figures 25 through 37 illustrate this approach; however, the actual values were calculated mathematically as described above.

Table VII summarizes the results of the fatigue study in terms of the Prot endurance limit to ultimate tensile strength ratio ( $E_p/UTS$ ). In the case of notched specimens twice the Prot endurance limit is used to describe the data ( $2E_{pn}/UTS$ ). Figure 4 illustrates the effect of tempering temperature on the fatigue properties of the nickel-molybdenum steel series. Typical microstructures of these steels are shown in Figures 5 through 24. The axial fatigue data determined for nickel-molybdenum steels at ASD are presented in Tables VIII and XI.

#### V. DISCUSSION

The effect of melting practice on fatigue properties is illustrated in Table X. This Table shows the data for nickel-molybdenum steels having ultimate tensile strengths in the 274 to 303 ksi range. The most fatigue-resistant material was provided by carbon-aluminum deoxidation practice. The efficacy of this technique is suggested by previous work in this area (WADC Technical Reports 58-289, September 1958, and 60-120, June 1960). An extensive

range of  $E_p/UTS$  values was exhibited by these materials. The upper limit of 0.500, characteristic of carbon-aluminum deoxidation, represents ultra-high fatigue strength. The lowest value, 0.328, provided by adding 0.30 per cent silicon to a carbon-aluminum deoxidized melt, is less than would be expected of commercial high-strength steels. The relative position of the remaining alloys is not easily explained, however. According to earlier research, fatigue strength could be related to the presence of nonmetallic inclusions, especially the larger ones. This correlation does not appear to apply in the case of the current steel series.

Representative metallographic samples of all tested materials were examined carefully (Figures 5 through 13). This series of photomicrographs illustrates inclusions characteristic of the various materials. It does not necessarily reflect either the average inclusion size or total content, however. A more accurate estimate of total inclusion content and distribution can be obtained at lower magnification, and this is presented in Figures 14 through 22. These steels can be broken down into three groups on the basis of total inclusion content. The first, or clean, group consists solely of steel RVC; this steel was prepared from high-purity raw materials by the consumable electrode arc-melting process and would be expected to be relatively free of inclusions. The second group might be described as moderately clean and includes steels 4, J, 1, 2A, H, and 3. Steel 2B was not examined in view of its similarity to 2A. Alumina, sulfide, and oxide and/or silicate inclusions were present in all samples of this group; the concentration of sulfides was considerably higher in alloys J and H. The final group was considered dirty, and was made up of steels DU and D10B.

The relative cleanliness was not indicated by conventional chemical analysis. The phosphorous content with one exception was less than 0.015 per cent which is generally taken as an acceptable value for high-quality steel. The amount of sulfur was higher, ranging from 0.015 to 0.022 per cent, except the RVC percentage of 0.010. The silicon content in the instances where it was not added intentionally was the same order of magnitude as that of sulfur, varying from 0.01 to 0.02 per cent with the exception of steel 1, which indicated 0.13 per cent. The effect of this higher silicon content was not evident. A variation in the remaining constituents (carbon, nickel, and molybdenum) would not be expected to exert a profound influence on cleanliness.

The relatively low  $E_p/UTS$  ratio of the consumable electrode-pure raw material heat (RVC) is of particular significance. Although this was the cleanest steel of the group, this was not reflected in fatigue performance. Air melting and standard deoxidation practice produced a more fatigue-resistant material than RVC even with more nonmetallics present in the microstructure. Steel D10 studied previously was prepared by air melting and carbon-aluminum deoxidation practice. This resulted in a "dirtier" heat than any of the current alloys (Figures 23 and 24) with respect to total inclusion content, yet an  $E_p/UTS$  ratio of about 0.6 was obtained for this steel at a tensile strength of 235 ksi. At a strength level comparable to RVC, an alloy D10 type gave an  $E_p/UTS$  ratio of 0.515. These differences in fatigue properties cannot be explained on the basis of metallic aspects of the microstructure. All of the materials under consideration proved to exhibit a normal quenched and tempered martensitic structure. Although some banding was noted,

there was nothing to suggest any significant difference in fatigue performance. The representative grain size range extended from about ASTM No. 6 to No. 7, and this degree of variation was not considered important.

The carbon-aluminum deoxidation practice appears to make a substantial contribution to fatigue properties, although its exact function is unclear. This effect appears to be reduced substantially when either consumable electrode vacuum arc or vacuum induction remelting operations are applied afterwards. A new and different set of equilibrium conditions was established during remelting, and this may explain the differences noted. Vacuum induction remelting was the more damaging of the two techniques. Arc remelting would be expected to yield a cleaner product as the higher arc temperatures would tend to promote greater oxide reduction through reaction with the carbon. The major benefit of vacuum induction remelting would be associated with a lowering of the gas content, although some degree of oxide reduction might occur. In practice, no benefits were obtained from remelting, however, as both processes resulted in reduced fatigue strength.

The nickel-molybdenum steel used was a simple composition never examined previously, and relatively high Prot fatigue values were obtained from this material prepared by standard deoxidation practice. The chemical composition is of considerable interest in this work. During the previous program, the highest  $E_p/UTS$  ratio for standard melting conditions, 0.434, was obtained on a tungsten-molybdenum steel tempered at 850°F having a tensile strength of 259 ksi. (This alloy was designated BB-X and was similar in composition to D10B.) In this instance, steel 1, melted in an analogous manner and tempered at 450°F, had an  $E_p/UTS$  ratio of 0.440 with a tensile strength of 282 ksi. This is a rather high value for this condition as compared to commercial AISI 4340, for example; it suggests that the composition of the basic steel alloy may have influenced or masked some of the effects of melting practice.

The consequence of silicon additions seemed equally complex. Silicon added after aluminum killing, in conjunction with carbon-aluminum deoxidation, had a less deleterious effect than the same addition made at the same time as the major alloy constituents. However, an air-melted heat was prepared with iron oxide and ferrosilicon additions in an effort to promote the formation of silicates. A high silicon content (steel DU, 0.73 per cent) and a relatively dirty microstructure resulted from this treatment. The  $E_p/UTS$  ratio was greater than for normal silicon addition prior to aluminum killing, however. The presence of silicon, as well as its distribution in the microstructure, is significant, although the relationships involved cannot be completely described. It appears, however, that any benefit silicon might contribute as an alloy addition, even under the most favorable circumstances, is more than overshadowed by the harmful effects of silicon-bearing non-metallics.

Two nickel-molybdenum steels were studied in both the notched and unnotched condition, and these results are summarized in Table XI. The  $2E_{pn}/E_p$  ratio is a standard method for comparing notched and unnotched properties and the carbon-aluminum specimens (2A and 2B) gave a  $2E_{pn}/E_p$  ratio of 0.907, while the material melted with iron oxide and ferrosilicon additions (DU) yielded a 1.058 value for the same ratio. A value of 1.00 is generally

taken to indicate good notched properties, and on this basis these steels were relatively insensitive to notching. Although both values were relatively high, the dirtier steel, DU, had a higher ratio. These results may reflect the large number of notches, resulting from inclusions, in the DU steels, especially as the 2A and 2B materials had significantly higher  $E_p/UTS$  and  $2E_{pn}/UTS$  ratios.

Axial fatigue techniques were also used to evaluate nickel-molybdenum steels 1 and 2B in the notched and unnotched condition. Only a limited number of specimens were available, and the data scatter was too great to permit quantitative comparisons of such effects of melting practice on notching.

The D10B specimens were prepared to determine the notch sensitivity of tungsten-molybdenum steels. During the previous program this composition (steel D10) showed excellent fatigue behavior in the unnotched condition. Chemical analyses and pertinent data are given in Table XII. The  $2E_{pn}/E_p$  ratio representing a 1225°F temper gives a value of 0.830 at a 235 ksi strength level, indicating a slight degree of notch sensitivity. The carbon content is significantly higher in the current alloy, 0.52 as compared to 0.45 per cent in the original. There are not sufficient data to draw a definite conclusion regarding the effect of carbon, but previous work has indicated that higher carbon contents tend to decrease the  $E_p/UTS$  ratio. Consequently, a comparison of notched and unnotched properties at a similar carbon level might yield a  $2E_{pn}/E_p$  ratio closer to 1.00.

Steel D10B was also tested after tempering at 1050°F. A lower tempering temperature was included to avoid the peak aging range (1100° to 1150°F); this resulted in a higher ultimate tensile strength and a slightly improved elongation (Table VII). The Prot endurance limit was raised markedly by this treatment, but the corresponding increase in tensile strength caused a slight reduction in the  $2E_{pn}/UTS$  ratio.

A summary of the standard deviations of the Prot fracture stress data for both high and low loading rates is given in Table XIII. The notched specimens demonstrated markedly lower standard deviations than their unnotched counterparts. This is the normal occurrence in fatigue testing and indicates that the presence of a notch has a greater effect on the scatter than any of the other variables. There does not appear to be any correlation between the unnotched deviations and either melting practice or fatigue strength, and this follows the general trend of the data obtained throughout this program.

The relationship between tempering temperature and fatigue strength was not uniquely defined in previous work, and this situation was not clarified definitively during the present program. Carbon-aluminum deoxidized material (steel 2A) was tempered at 1000° as well as 450°F. An appreciable improvement in the  $E_p/UTS$  ratio resulted, increasing from 0.500 to 0.555. The overall data relating tempering temperature and fatigue properties (Figure 4) indicate that the Prot endurance limit is not affected to any appreciable extent. The  $E_p/UTS$  and  $2E_{pn}/UTS$  ratios increase with increasing tempering temperature; however, this seems to be a direct function of the decrease in ultimate tensile strength with increasing tempering temperature. If fatigue

strength is evaluated solely on the basis of the  $E_p/UTS$  ratios, then increasing tempering temperature appears to have a beneficial effect. The current data are not sufficient to establish a more valid relationship, however.

The higher carbon versions of the D10B type tungsten-molybdenum steel indicated high tensile and yield strengths with relatively low elongation values on room-temperature testing. Austenitizing temperatures of 1950° and 2050°F were utilized for hot tensile studies and the higher temperature treatment provided higher strengths and lower elongations. On the basis of previous experience, 2050° and 2200°F were selected for austenitizing the hot tensile specimens as the resistance to softening in these steels increases with increasing austenitizing temperature. The hot tensile data at 700° and 900°F tended to show the strengthening effect of higher austenitizing temperature for both steels S-6 and S-8, and the elongation values were correspondingly lowered by the higher temperature treatment. Approximate values were obtained for the modulus of elasticity at room and elevated temperatures as shown below.

<u>Modulus of Elasticity,</u> <u>1000 ksi</u>	<u>Test Temperature,</u> <u>°F</u>
31-33	72 (RT)
25-27	700
22-24	900

These data were obtained during the tensile testing of the S-6 and S-8 steels. The individual steel data were not considered separately, as this presentation clearly indicated the effect of temperature on the elastic modulus.

The stress-rupture specimens were austenitized at 2050°F to obtain higher ductility and double tempered at 1050°F, well above the test temperature. The stress-rupture data indicated the presence of notch sensitivity, which was evident by failures in the threaded sections as the time at temperature increased. This behavior was related to previously noted aging behavior in the tempering range. While this generally occurred at higher temperatures, apparently extended time at lower temperatures can produce a similar effect.

The over-all differences in composition between steel S-6 and S-8 were too great to permit an accurate evaluation of the effect of carbon content. Carbon would be expected to exert a larger effect than the other alloy elements, however; and on this basis the increase in carbon content from 0.62 to 0.73 per cent did not have a significant effect on either hot tensile or stress-rupture properties.

## VI. SUMMARY

The effect of melting practice on the Prot fatigue properties of a nickel-molybdenum high-strength steel was investigated. Various preparatory techniques were utilized involving induction melting in air with standard and special carbon-aluminum deoxidation techniques, vacuum arc and vacuum induction remelting of specially deoxidized material, and vacuum arc melting of high-purity raw materials. Further studies included the consequence of silicon additions, before and after aluminum killing, as applied to special carbon-aluminum deoxidation practice, and silicate-bearing steel prepared by adding iron oxide and silicon dioxide during conventional air induction melting.

The experimental ingots, varying from 15 to 60 lb were hot forged into 3/4 in. rounds, and machined into notched and unnotched cylindrical R. R. Moore fatigue bars. These specimens were austenitized at 1525°F, oil quenched, and with one exception tempered at 450 to 600°F to develop ultimate tensile strengths in the 250 to 300 ksi range. The exception was tempered at 1000°F to determine fatigue properties at a lower tensile strength level. The Prot accelerated technique was used throughout this program. These results showed that the special carbon-aluminum deoxidation practice was the most effective in raising the fracture stress level, and  $E_p/UTS$  ratios of 0.500 and 0.555 were determined at tensile strength levels of 274 and 200 ksi, respectively; these values represent a considerable improvement over commercial high-strength steels at comparable strength levels. All of the remaining techniques were inferior to air melting with standard deoxidation practice, including vacuum arc melting of pure raw materials. Remelting specially deoxidized material by vacuum arc and vacuum induction processes resulted in a significant loss of fatigue strength. The effect of silicon additions was dependent upon the manner in which it was added; a 0.30 per cent silicon addition after the aluminum killing sequence was far less damaging than a similar addition prior to killing.

Notched Prot evaluations were made of two nickel-molybdenum steels, and one tungsten-molybdenum steel which was studied in the unnotched condition during the previous program. Notching had little effect on the nickel-molybdenum steels—one prepared by carbon-aluminum deoxidation practice and the other a high-silicon steel made with iron oxide and silicon dioxide additions—based on  $2E_{pn}/E_p$  ratios of approximately 1.00. These data indicate that the effect of melting practice is far less significant in the case of notched fatigue specimens. The carbon-aluminum deoxidized tungsten-molybdenum steel was slightly notch sensitive giving a  $2E_{pn}/E_p$  ratio of 0.830 at a 235 ksi tensile strength level.

The elevated temperature properties of two D10 type tungsten-molybdenum steels containing 0.73 and 0.62 per cent carbon were investigated. Satisfactory tensile properties were obtained at temperatures of 700° and 900°F, and the difference in carbon content between the two steels did not have a significant effect on elevated temperature behavior. The elastic modulus decreased from 31 to 33 million psi at room temperature to 25 to 27 million psi

at 700°F and 22 to 24 million psi at 900°F. Stress rupture tests were performed at 900°F, and both steels demonstrated the effects of notch sensitivity with increasing time at temperature.

## VII. CONCLUSIONS

### A. Effect of Melting Practice

Special carbon-aluminum deoxidation practice applied to induction-air melted silicon-free steel provided a substantial increase in fatigue strength as compared to standard induction melting techniques. At strength levels of 274 and 200 ksi,  $E_p/UTS$  ratios of 0.500 and 0.555, respectively, were determined; this represents a significant improvement over commercial steels of similar tensile strength. Vacuum arc and vacuum induction remelting of the specially deoxidized steel had an adverse effect on fatigue properties and these techniques proved to be inferior to conventional practice. High-purity raw materials subjected to consumable electrode vacuum arc melting operations produced higher fatigue strengths than the remelted steels, but lower than those prepared by induction melting. There was no apparent correlation between Prot fatigue properties and cleanliness based on either total inclusion content or the distribution of inclusion sizes. The carbon-aluminum deoxidation process made the most outstanding contribution to improving fatigue properties at high strength levels, and this effect outweighed cleanliness or any other consequence of melting.

### B. Notched Properties

Nickel-molybdenum steels prepared by carbon-aluminum deoxidation and a silicate-forming technique were shown to have good notched properties on the basis of  $2E_{pn}/E_p$  ratios of approximately 1.00. Notched fatigue strength appeared to be independent of melting practice and inclusion content and distribution, suggesting that these factors were only of secondary importance in the presence of a notch.

The notched properties of a tungsten-molybdenum steel, analogous to materials investigated in the unnotched condition during the previous program, indicated a minor degree of notch sensitivity. At a similar tempering temperature, 1225°F, a  $2E_{pn}/E_p$  ratio of 0.830 was obtained; the actual values were 117 and 141 ksi, for the notched and unnotched materials, respectively. At a lower tempering temperature, 1050°F, the  $2E_{pn}$  value increased to 132 ksi, indicating a probable decrease in notch sensitivity in this region.

## C. Effect of Silicon

Tentatively, the results of this work indicate that silicon tends to have a detrimental effect on fatigue strength. The manner in which silicon was introduced was of considerable importance, and the best technique consisted of adding the silicon after the aluminum killing sequence in preparing a carbon-aluminum deoxidized heat. The presence of silicon in the metallic phases of the structure did not have any noticeable results, and the over-all effect suggests the complete absence of silicon for optimum fatigue properties.

## D. Effect of Tempering Temperature

Increasing tempering temperature caused a corresponding increase in the  $E_p/UTS$  ratios of nickel-molybdenum steel alloys. This effect appeared to be more closely related to the decrease in ultimate tensile strength than any increase in the Prot endurance limit, however.

## E. Elevated Temperature Properties of Tungsten-Molybdenum Steels

Satisfactory tensile behavior was noted in the 700° to 900°F range for two high-carbon tungsten-molybdenum steels. Hot tensile properties appeared to be unaffected by carbon content in the 0.62 to 0.72 per cent region. Elastic modulus values of 25 to 27 million and 22 to 24 million psi were measured at 700° and 900°F, respectively. Both steels indicated notch-sensitive behavior during stress-rupture testing at 900°F with increasing time at temperature.

## VIII. BIBLIOGRAPHY

1. H. N. Cummings, F. B. Stulen, and W. C. Schulte, "Research on Ferrous Materials Fatigue," WADC Technical Report 58-43, April 1958.
2. J. I. Fisher and J. P. Sheehan, "The Effect of Metallurgical Variables on the Fatigue Properties of AISI 4340 Steel Heat-Treated in the Tensile Strength Range 260,000-310,000 psi," WADC Technical Report 58-289, September 1958.
3. H. B. Nudelman and J. P. Sheehan, "Development of Ultra-High Strength, Temper-Resistant Steels Designed for Improvement of Fatigue Properties Through Relief of Residual Stress," WADC Technical Report 59-86, June 1959.
4. H. B. Nudelman and J. P. Sheehan, "Study of Fatigue Properties of Ultra-High Strength Steel," WADD Technical Report 60-120.

TABLE I  
COMPOSITION OF EXPERIMENTAL STEELS

Steel	Melting Practice	Composition								
		C	W	Mo	V	Mn	Ni	Si	S	P
1	Air melt, std. deox.	.44	--	1.06	--	.050*	1.98	.13	.021	.013
2A	Air melt, C-Al deox.	.43	--	.94	--	.050*	1.83	.01	.015	.013
2B	Air melt, C-Al deox.	.47	--	1.12	--	.050*	2.25	.01	.016	.013
3	Air melt, C-Al deox. with 0.30% Si addition before Al killing	.44	--	1.04	--	.050*	1.98	.32	.021	.013
4	Air melt, C-Al deox. with 0.30% Si addition after Al killing	.55	--	1.12	--	.050*	2.09	.27	.015	.012
J	Vacuum-arc remelt- ing of condition 2	.50	--	1.07	--	.050*	2.04	.02	.020	.012
H	Vacuum-induction remelting of con- dition 2	.52	--	1.04	--	.050*	2.04	.02	.015	.015
RVC	Vacuum-arc melt- ing of high purity raw materials	.52	--	1.04	--	.050*	2.12	.02	.010	.005
DU	Air melt, with iron oxide and ferrosilicon additions	.49	--	.94	--	.050*	1.95	.73	.022	.012
D10B	Air melt, C-Al deox.	.52	1.96	1.08	.45	.96	--	.07	.028	.014

\* Nominal Mn addition

Cb is present in steel D10B at a 0.10% level

TABLE II

PRELIMINARY SHEET TENSILE PROPERTIES  
OF NICKEL-MOLYBDENUM STEEL

Tempering Temp. °F	UTS, ksi	YS, ksi	Elong, %	Hardness, R <sub>c</sub>
450	319	274	4	55
550	281	250	5	53

Composition: C 0.57, Ni 2.10, Mo 1.12%

Austenitizing temperature: 1525°F

TABLE III  
FATIGUE BAR TENSILE DATA

Steel	Tempering Temp. °F	UTS, ksi	Elong,* %	Hardness, R <sub>c</sub>
1	450	282	9.0-11.0	52
2A	450	274	9.0-11.0	52
2A	1000	200	15.0	41
2B	475	280	8.0	52-53
3	450	302	7.0-9.0	53
4	500	303	7.0	53
J	475	300	7.0-9.0	53-54
H	500	276	10.0	52
RVC	475	280	10.0-11.0	53
DU	550 + 600	298	7.0	53
D10B	1050	282	6.0	54
D10B	1225	238	5.0-6.0	48

\* Elongations were determined over a 1 in. gage length.  
All tempering times were 1 hr.  
All data were obtained on unnotched specimens.  
Austenizing temperatures: D10B 2050°F; all other  
steels 1525°F.

TABLE IV

ROOM-TEMPERATURE TENSILE DATA FOR STEELS S-6 AND S-8

Austenitizing Temp. °F	Tempering Temp. °F	UTS, ksi	YS, ksi	Elong., %
<u>Steel S-6</u>				
1950	1050	297	284	4.5
1950	1050	297	282	4.0
1950	1150	284	279	4.0
1950	1150	284	278	4.5
2050	1050	306	289	---
2050	1050	304	284	2.0
2050	1150	297	287	1.5
<u>Steel S-8</u>				
1950	1050	291	273	5.5
1950	1050	289	271	4.5
1950	1150	284	278	4.0
1950	1150	284	274	4.0
2050	1050	297	274	3.0
2050	1050	297	278	3.0
2050	1150	297	286	2.0
2050	1150	297	286	1.5

All samples were tempered for 1 + 1 hours.

Composition:

Steel	C	Mn	W	Mo	V
S-6	0.73	0.74	1.44	0.95	0.57
S-8	0.62	0.68	1.57	1.16	0.48

TABLE V  
ELEVATED TEMPERATURE TENSILE DATA  
FOR STEELS S-6 AND S-8

Test Temp., °F	Austenitizing Temp., °F	Tempering Temp., °F	UTS, ksi	YS, ksi	Elong., %
<u>Steel S-6</u>					
700	2050	1050	243	207	13.5
		1150	230	205	9.5
	2200	1050	250	211	2.5
		1150	237	205	5.5
900	2050	1050	216	185	11.0
		1150	198	178	10.0
	2200	1050	215	196	*
		1150	217**	203**	5.0
<u>Steel S-8</u>					
700	2050	1050	241	213	12.5
		1150	234	204	11.5
	2200	1050	249	204	6.5
		1150	238	210	4.0
900	2050	1050	212	199	9.0
		1150	196	172	10.5
	2200	1050	220	193	3.5
		1150	210	187	4.0

\* Fractured in threads

\*\* Tested at approximately 825°F

YS values were based on 0.2 per cent offset. Elongations were measured over a 1 in. gage length.

TABLE VI

900°F STRESS-RUPTURE DATA FOR STEELS S-6 AND S-8

Stress, ksi	Time to Rupture, hr	
	Steel S-6	Steel S-8
200	0.45	1.40
175	1.10	1.40
150	9.50	16.50*
130	38.10*	33.50*
120	15.90*	29.70*

\* Fractured in threads.

All specimens were oil quenched from 2050°F and tempered at 1050°F for 1 + 1 hr.

TABLE VII  
SUMMARY OF FATIGUE DATA

Steel	Tempering Temp., °F	UTS, ksi	$E_p$ , ksi	$2E_{pn}$ , ksi	$E_p/UTS$ or $2E_{pn}/UTS$	Elong. %
1	450	282	124	--	.440	9.0-11.0
2A	450	274	137	--	.500	9.0-11.0
2A	1000	200	111	--	.555	15.0
2B	475	280	--	127	.454	8.0
3	450	302	99.1	--	.328	7.0-9.0
4	500	303	131	--	.432	7.0
J	475	300	116	--	.387	7.0-9.0
H	500	276	94.0	--	.341	10.0
RVC	475	280	119	--	.425	10.0-11.0
DU	550 + 600	298	120	--	.403	7.0
DU	550 + 600	298	--	127	.426	7.0
D10B	1050	282	--	132	.468	6.0
D10B	1225	238	--	117	.492	5.0-6.0

All UTS and elong. values were determined on unnotched specimens.  
All tempering times were 1 hr.

TABLE VIII

## NOTCHED AXIAL FATIGUE DATA

Specimen No.	Stress, ksi	Cycles
1-11	50.0	12,082,500
1-13	52.5	11,760,300 NF
1-15	53.75	70,100
1-12	55.0	164,700
1-18	55.0	73,100
1-16	55.0	13,000
1-17	57.5	30,600
1-10	60.0	38,000
1-14	62.5	32,200
2B-11	45.0	205,600
2B-11	47.5	12,080,300 NF
2B-16	48.75	7,558,600
2B-17	50.0	1,402,200
2B-15	52.5	291,300
2B-18	55.0	46,500
2B-10	57.5	71,700
2B-12	60.0	27,800

NF-no failure

TABLE IX  
UNNOTCHED AXIAL FATIGUE DATA

Specimen No.	Stress, ksi	Cycles
1-3	105.0	12,334,700 NF
1-5	107.5	1,058,100
1-6	110.0	1,595,400
1-9	112.5	18,200
1-4	112.5	12,469,200 NF
1-1	115.0	78,200
1-7	117.5	471,300
1-2	120.0	8,700
2B-8	110.0	1,666,400
2B-3	111.25	207,900
2B-1	111.25	166,400
2B-7	112.5	137,100
2B-4	115.0	366,200
2B-6	117.5	68,100
2B-9	120.0	275,000
2B-2	122.5	137,100

NF-no failure

TABLE X  
MELTING PRACTICE RANKED BY FATIGUE STRENGTH  
AT SIMILAR UTS LEVELS

Steel	Melting Practice	$E_p/UTS$
2A	Air melt, C-Al deox.	.500
2B	Air melt, C-Al deox.	.454*
1	Air melt, std deox.	.440
4	Air melt, C-Al deox. with 0.30% Si addition after Al killing	.432
DU	Air melt, with iron oxide and ferrosilicon additions	.426*
RVC	Vacuum arc melting of pure raw materials	.425
DU	Air melt, with iron oxide and ferrosilicon additions	.403
J	Vacuum arc remelting of C-Al deox.	.387
H	Vacuum induction remelting of C-Al deox.	.341
3	Air melt, C-Al deox. with 0.30% Si addition	.328

\*  $2E_{pn}/UTS$  value

UTS range 274 to 303 ksi; tempering range 450° to 600°F.

TABLE XI

## NOTCHED PROPERTIES OF NICKEL-MOLYBDENUM STEELS

Steel	Condition	Tempering Temp., °F	UTS,	$E_p$ ksi	$2E_{pn}$ , ksi	$E_p/UTS$ or $2E_{pn}/UTS$	$2E_{pn}/E_p$
2A	Unnotched	450	274	137	--	.500	.907
2B	Notched	475	280	--	127	.454	
DU	Unnotched	550 + 600	298	120	--	.403	1.058
DU	Notched	550 + 600	298	--	127	.426	

TABLE XII

NOTCHED PROPERTIES OF TUNGSTEN-MOLYBDENUM STEELS

Steel*	Tempering Temp., °F	UTS, ksi	$E_p$ , ksi	$2E_{pn}$ , ksi	$E_p/UTS$ or $2E_{pn}/UTS$	$2E_{pn}/E_p$
D10	1225	235	141	--	.600	
D10B	1225	238	--	117	.492	.830
D10B	1050	282	--	132	.468	--

\*

Composition:

	C	W	Mo	V	Mn
D10 +	.45	1.91	1.02	.44	.81
D10B++	.52	1.96	1.08	.45	.96

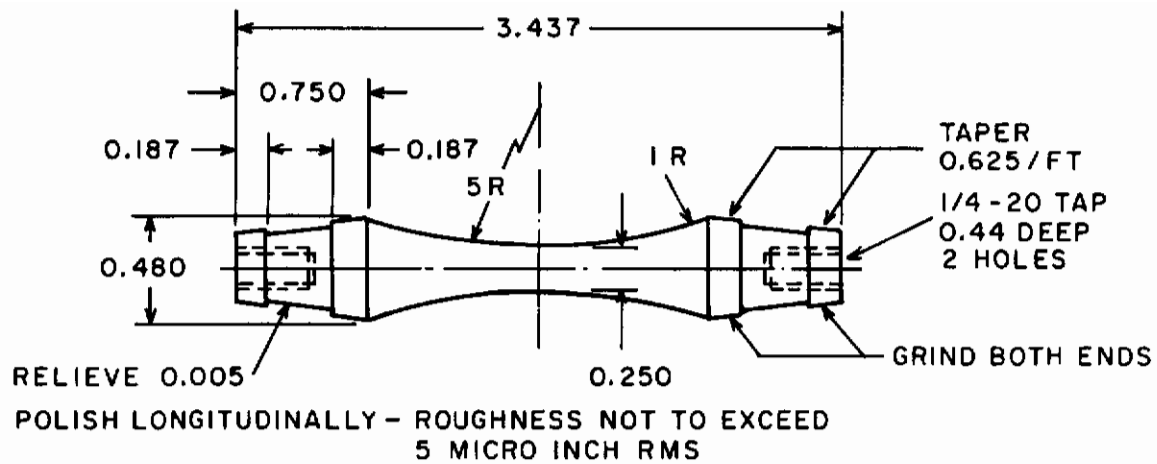
+ Unnotched specimens from previous program

++ Notched specimens from current program

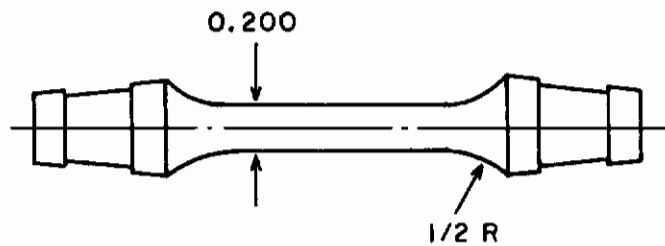
TABLE XIII

STANDARD DEVIATION OF PROT FRACTURE STRESS DATA

Steel	Specimen Type	Tempering Temperature (1 + 1 hr), °F	Standard Deviation of Prot Fracture Stress, ksi	
			Low Rate	High Rate
1	smooth	450	10.9	11.4
2A	smooth	450	12.6	7.7
2A	smooth	1000	4.1	4.7
3	smooth	450	19.3	14.5
4	smooth	500	16.4	24.8
J	smooth	475	7.3	10.4
H	smooth	500	12.8	10.3
RVC	smooth	475	11.0	3.6
DU	smooth	550 + 600	11.6	5.3
2B	notched	475	4.3	2.9
DU	notched	550 + 600	1.8	1.7
D10B	notched	1050	3.2	2.9
D10B	notched	1225	3.6	1.7

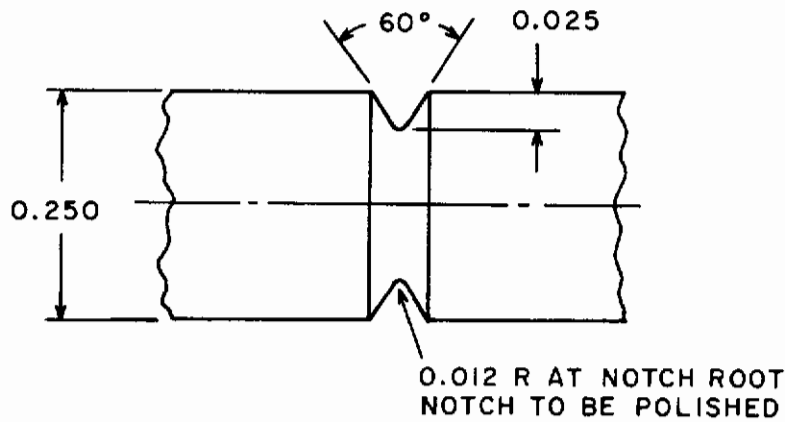


STANDARD R.R. MOORE SPECIMEN



ALL OTHER DIMENSIONS AND DETAILS AS  
PER STANDARD SPECIMEN SHOWN ABOVE

CYLINDRICAL R.R. MOORE SPECIMEN DETAIL



NOTE: CONCENTRICITY WITHIN 0.002 FOR ALL SPECIMENS

NOTCHED SPECIMEN DETAIL

FIG. 1 R.R. MOORE ROTATING BEAM FATIGUE SPECIMENS.

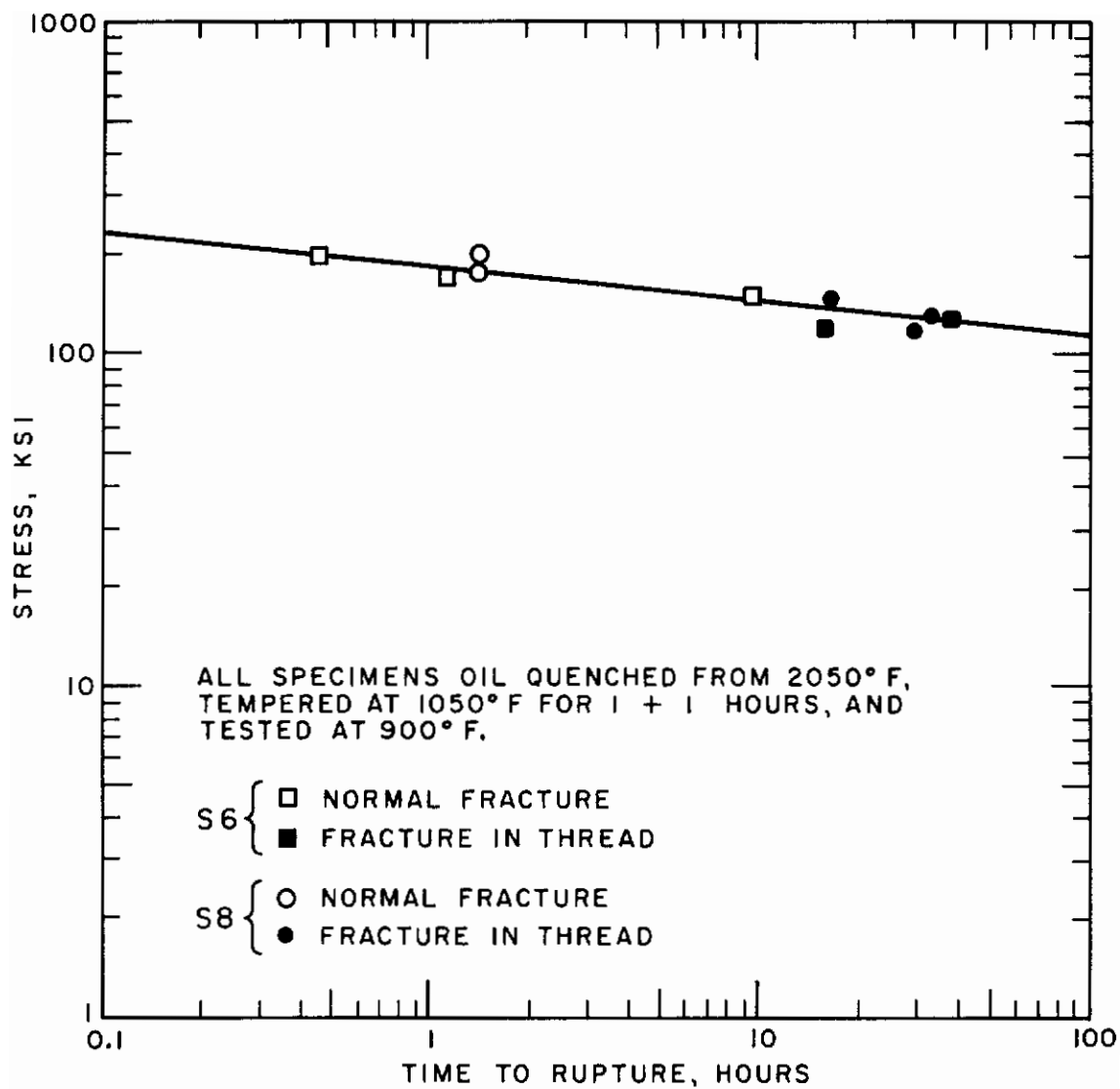


FIG. 2 STRESS-RUPTURE DIAGRAM FOR STEELS S6 AND S8.

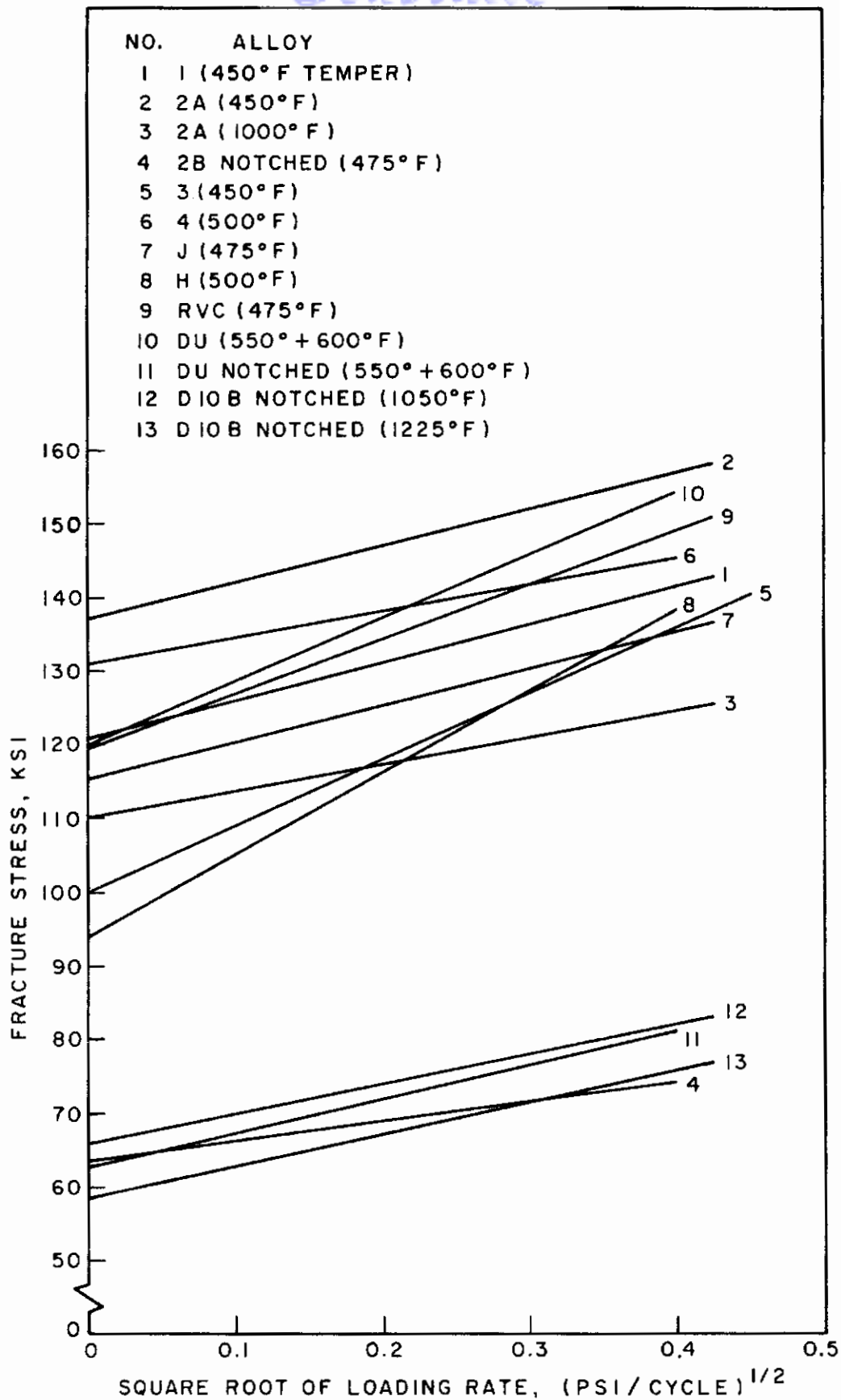


FIG.3 SUMMARY OF FATIGUE DATA.

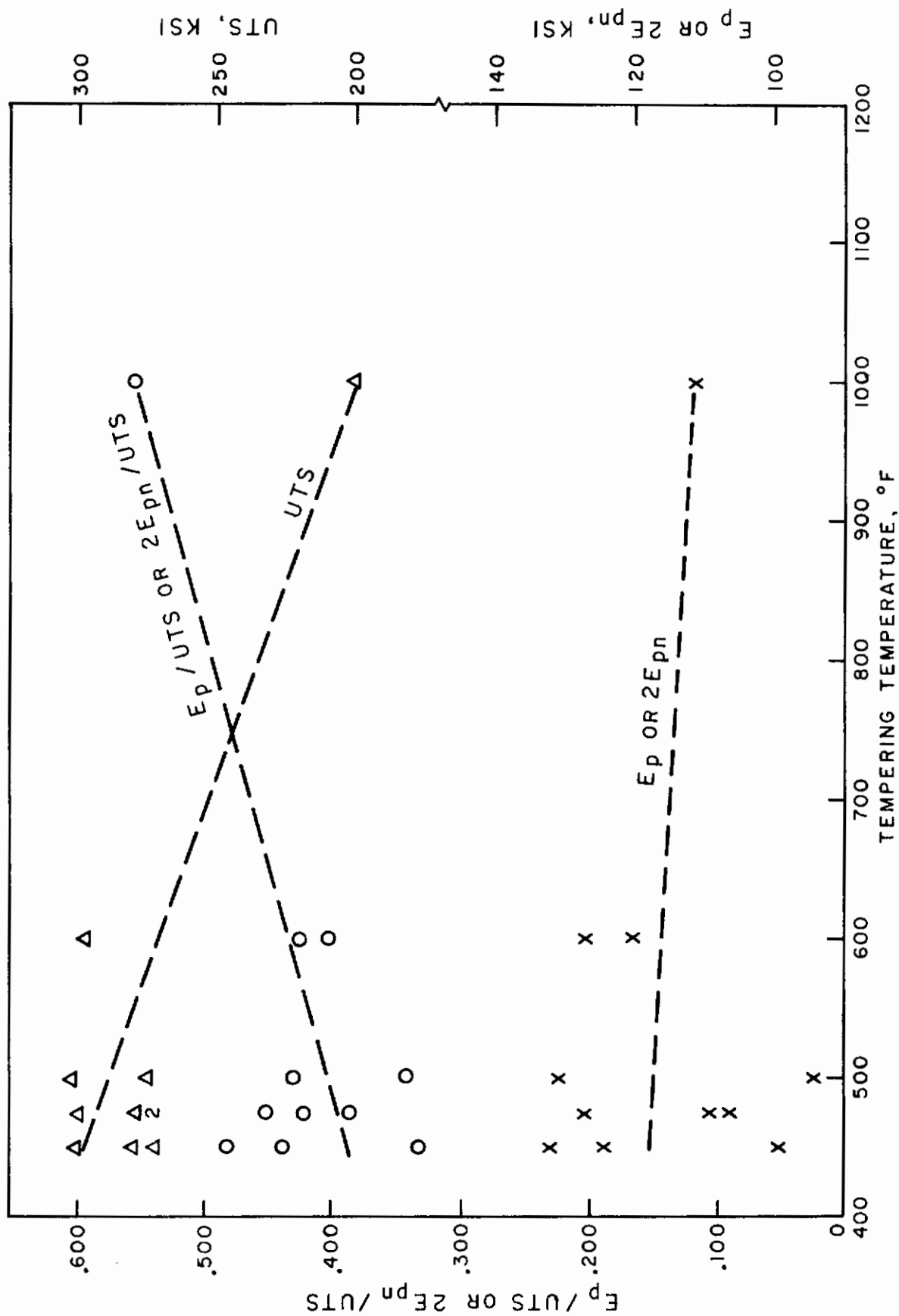
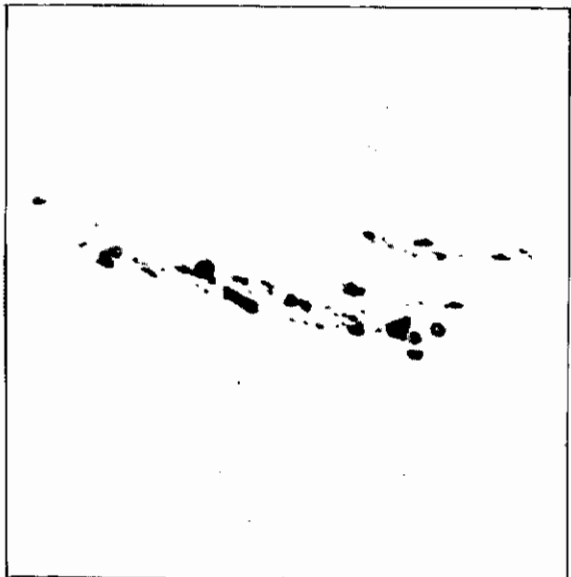


FIG. 4 THE EFFECT OF TEMPERING TEMPERATURE ON THE FATIGUE PROPERTIES OF Ni-Mo STEEL.

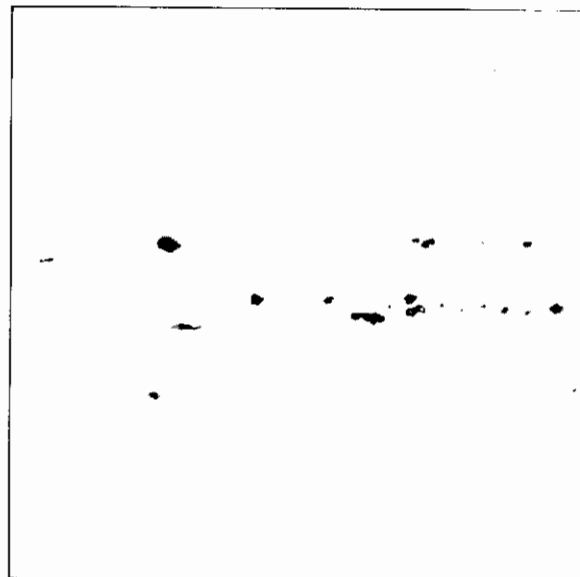
# Contrails



500X

Figure 5

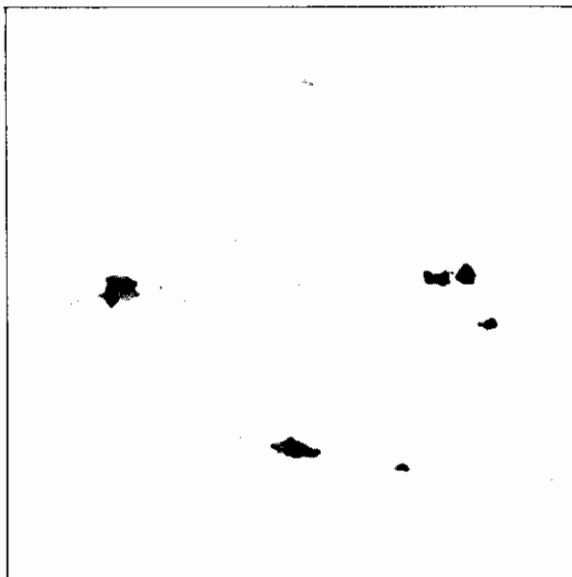
Steel 1 at High Magnification. Air Melt, Standard Deoxidation.



500X

Figure 6

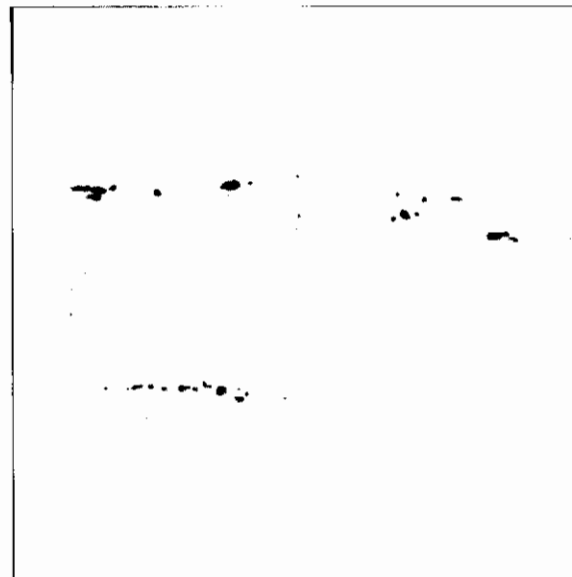
Steel 2A at High Magnification. Air Melt, C-Al Deoxidation.



500X

Figure 7

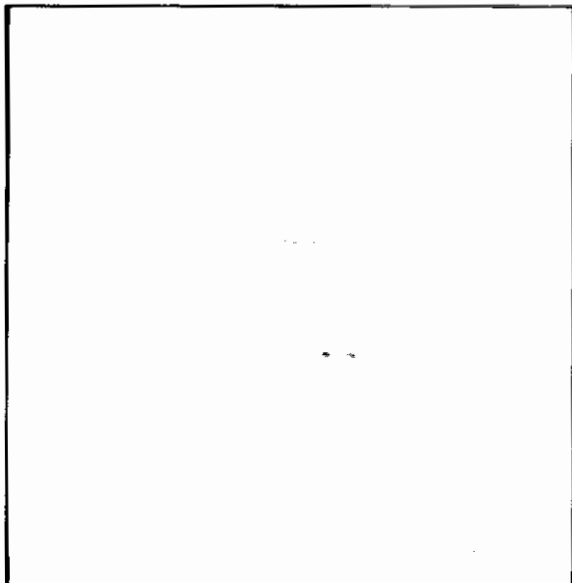
Steel 3 at High Magnification. Air Melt, C-Al Deoxidation with 0.30% Si Addition.



500X

Figure 8

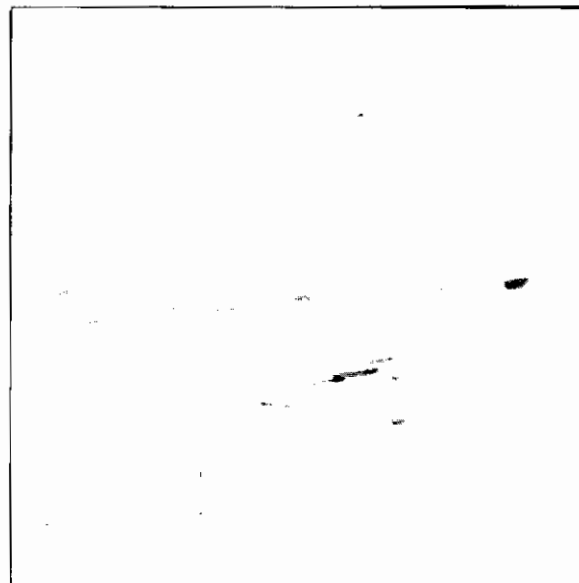
Steel 4 at High Magnification. Air Melt, C-Al Deoxidation with Si Addition after Al Killing.



500X

Figure 9

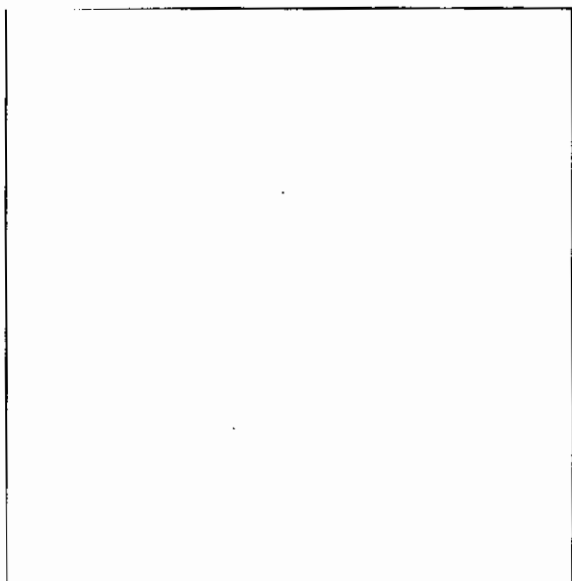
Steel J at High Magnification.  
Vacuum Arc Remelting of Alloy  
2A Type.



500X

Figure 10

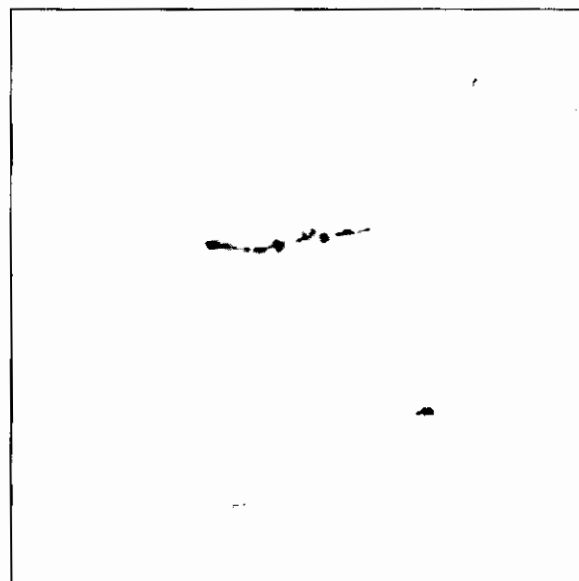
Steel H at High Magnification.  
Vacuum Induction Remelting of  
Alloy 2A Type.



500X

Figure 11

Steel RVC at High Magnification.  
Vacuum Arc Melting of Pure Raw  
Materials.



500X

Figure 12

Steel DU at High Magnification.  
Air Melt with Iron Oxide and  
Ferrosilicon Additions.

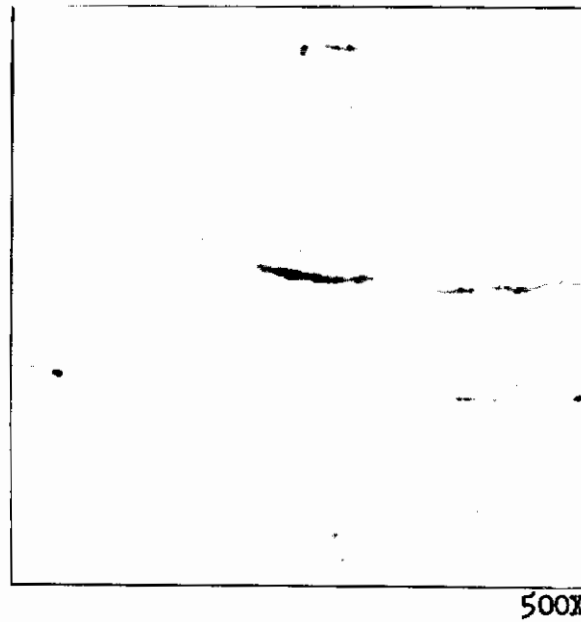
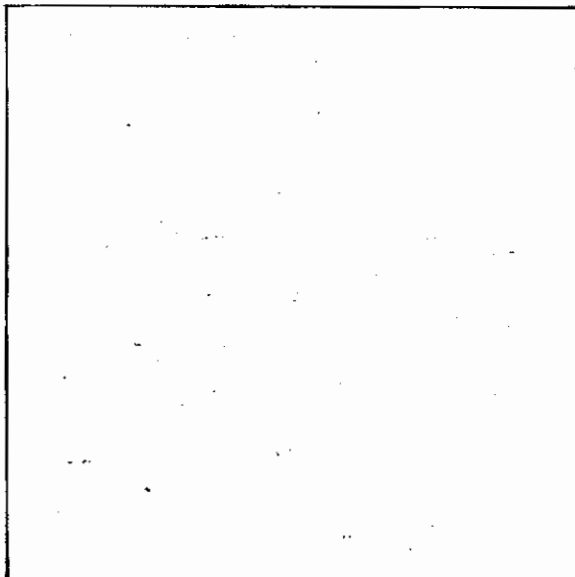


Figure 13

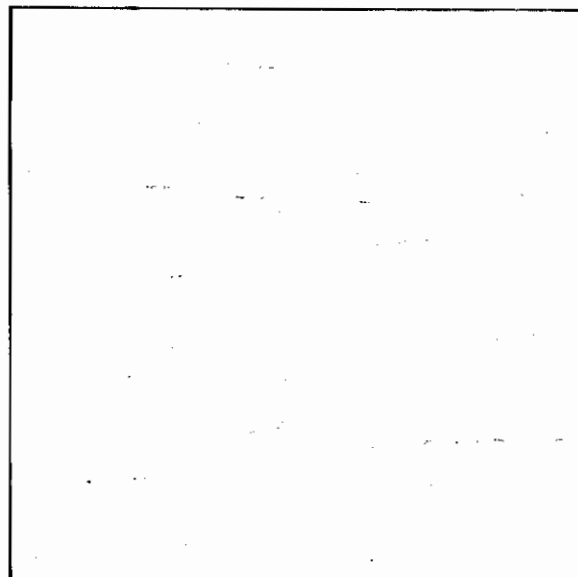
Steel D10B at High Magnification. Air  
Melt, C-Al Deoxidation.



50X

Figure 14

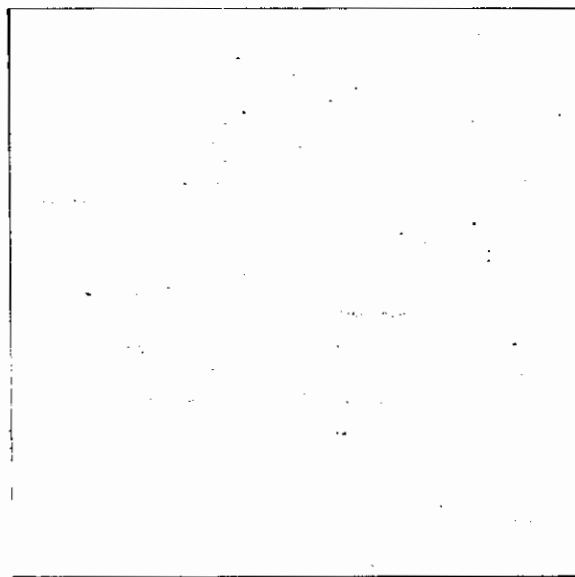
Steel 1, Air Melt, Standard  
Deoxidation.



50X

Figure 15

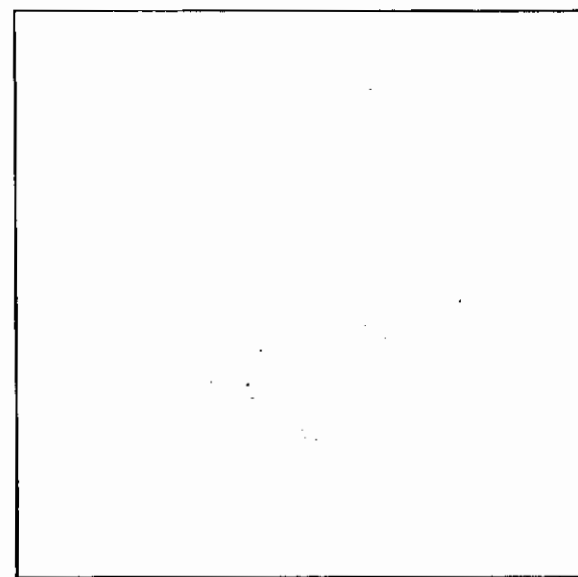
Steel 2A, Air Melt, C-Al Deoxida-  
tion.



50X

Figure 16

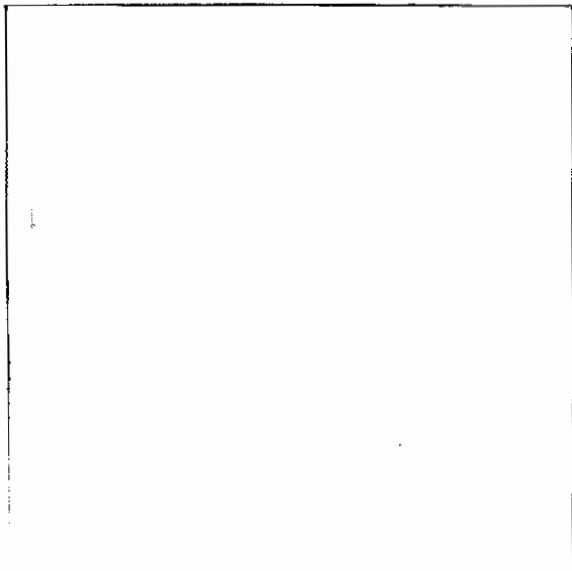
Steel 3, Air Melt, C-Al Deoxidation  
with 0.30% Si Addition.



50X

Figure 17

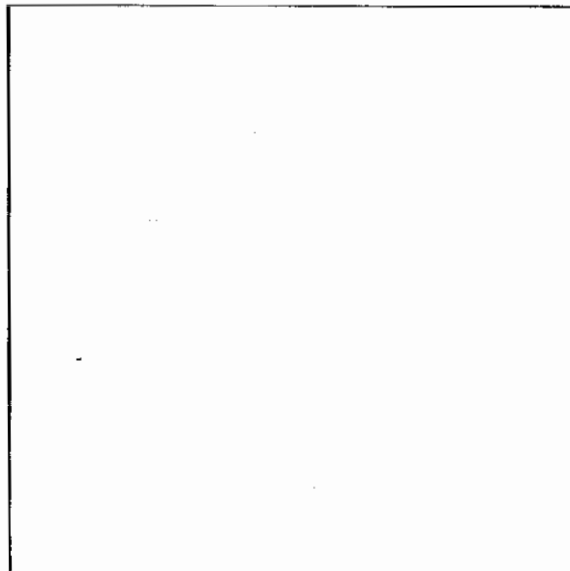
Steel 4, Air Melt, C-Al Deoxidation  
with 0.03% Si Addition after Al  
Killing.



50X

Figure 18

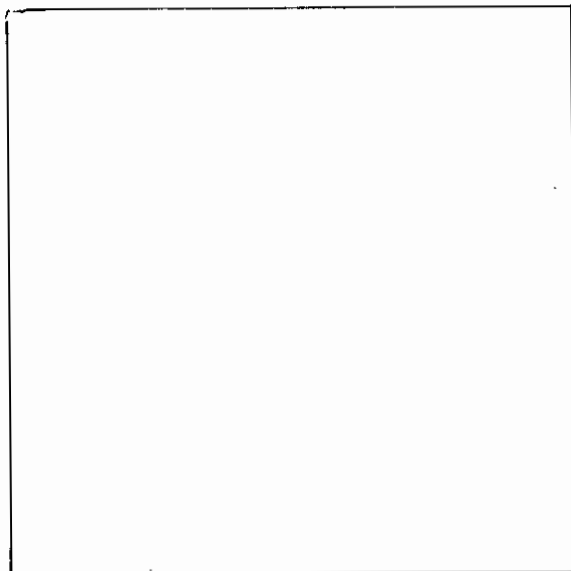
Steel J, Vacuum Arc Remelting of Alloy 2A Type.



50X

Figure 19

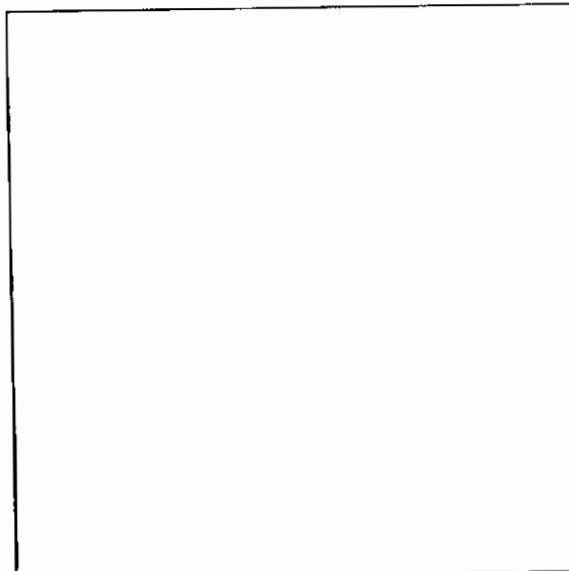
Steel H, Vacuum Induction Remelting of Alloy 2A Type.



50X

Figure 20

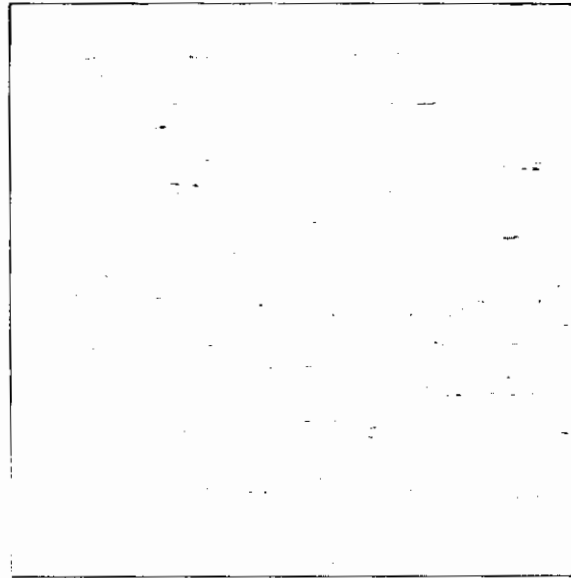
Steel RVC, Vacuum Arc Melting of Pure Raw Materials.



50X

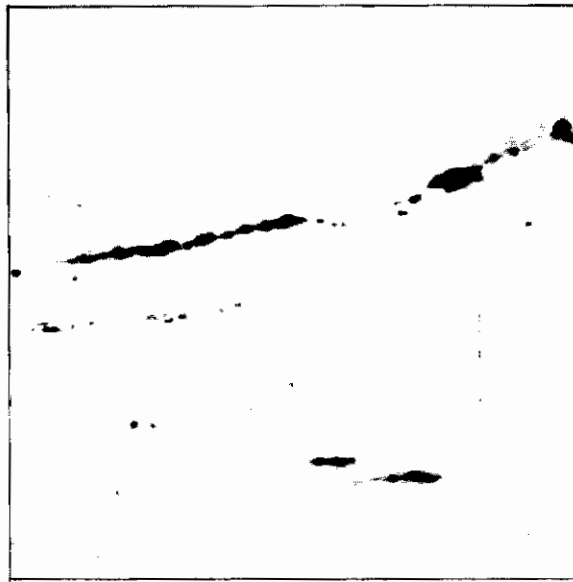
Figure 21

Steel DU, Air Melt with Iron Oxide and Ferrosilicon Additions.



50X

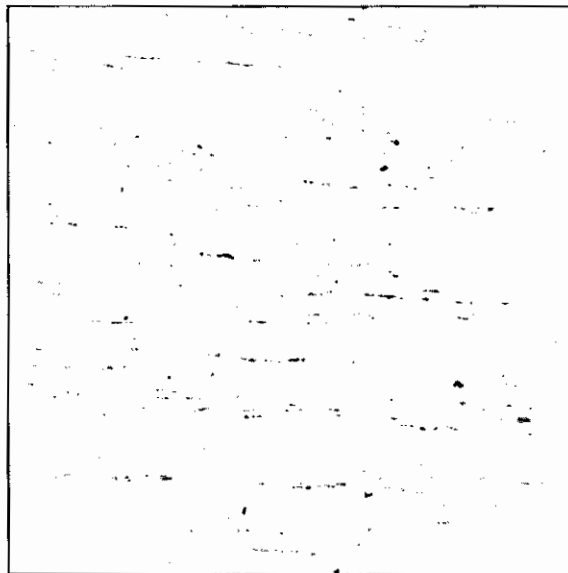
**Figure 22**  
**Steel D10B, Air Melt, C-Al Deoxidation.**



500X

Figure 23

Steel D10 at High Magnification.  
Air Melt, C-Al Deoxidation.



50X

Figure 24

Steel D10, Air Melt, C-Al Deoxidation.

APPENDIX I  
DETAILED PROT TESTING DATA

TABLE XIV

FATIGUE DATA, STEEL 1, 450°F TEMPER

Specimen No.	Rate ( $\alpha$ ), psi/cycle	Rate $1/2$ ( $\alpha$ ) $1/2$	Failure Stress, ksi
<u>High Rate</u>			
1-6	.159	.399	138
1-15	.120	.346	132.5
1-10	.116	.340	128.5
1-8	.115	.374	140
1-4	.156	.395	156.5
1-3	.157	.396	125
1-11	.156	.395	138
1-20	.155	.394	160.5
1-18	.158	.397	148
Average		.382	140.8
<u>Low Rate</u>			
1-14	.0143	.119	149.5
1-16	.0141	.119	109
1-7	.0098	.099	127.5
1-9	.0085	.092	122
1-1	.0125	.112	138
1-19	.0123	.110	133
1-12	.0182	.135	125
1-2	.0182	.135	134
1-14	.0122	.110	120
Average		.115	128.6

TABLE XV

FATIGUE DATA, STEEL 2A, 450°F TEMPER

Specimen No.	Rate ( $\alpha$ ), psi/cycle	Rate $1/2$ ( $\alpha$ ) $1/2$	Failure Stress, ksi
<u>High Rate</u>			
2A-10	.152	.389	149.5
2A-19	.148	.385	149.5
2A-8	.145	.381	163
2A-5	.145	.381	164
2A-3	.145	.381	156.5
2A-14	.146	.382	167
2A-1	.145	.381	163
2A-18	.152	.390	145
2A-17	.148	.385	149
Average		.384	156.3
<u>Low Rate</u>			
2A-16	.0141	.119	118.5
2A-7	.0139	.118	159
2A-6	.0139	.118	132.5
2A-15	.0140	.118	164
2A-11	.0121	.110	146
2A-13	.0131	.114	141
2A-9	.0116	.108	143
2A-12	.0105	.102	141
2A-4	.0117	.108	140
Average		.113	142.8

TABLE XVI

FATIGUE DATA, STEEL 2A, 1000°F TEMPER

Specimen No.	Rate (a), psi/cycle	Rate $1/2$ (a) $1/2$	Failure Stress, ksi
<u>High Rate</u>			
2A-21	.155	.394	127
2A-24	.130	.360	127.5
2A-29	.143	.378	127
2A-28	.147	.383	126
2A-25	.134	.366	121
2A-36	.136	.367	129
2A-27	.155	.394	116
2A-38	.121	.348	116
2A-23	.131	.362	125
Average		.372	123.8
<u>Low Rate</u>			
2A-37	.0138	.117	115
2A-22	.0135	.116	120
2A-34	.0140	.118	106
2A-36	.0105	.102	114
2A-32	.0116	.107	113
2A-35	.0113	.106	114.5
2A-33	.0113	.106	120
2A-26	.0102	.101	120
2A-39	.0116	.108	113
2A-31	.0116	.108	113
Average		.109	114.8

TABLE XVII

FATIGUE DATA, STEEL 2B NOTCHED, 475°F TEMPER

Specimen No.	Rate ( $\alpha$ ), psi/cycle	Rate $1/2$ ( $\alpha$ ) $1/2$	Failure Stress, ksi
<u>High Rate</u>			
2B-2	.137	.370	72.5
2B-17	.148	.384	74.0
2B-20	.150	.387	76.0
2B-11	.148	.384	68.5
2B-19	.147	.383	73.0
2B-5	.150	.387	73.0
2B-3	.150	.387	74.5
2B-4	.146	.382	71.5
2B-9	.149	.386	79.0
2B-7	.151	.389	78.5
Average		.384	74.0
<u>Low Rate</u>			
2B-18	.0116	.108	54.5
2B-1	.0127	.113	68.0
2B-10	.0122	.110	69.0
2B-12	.0125	.112	66.0
2B-8	.0125	.112	69.5
2B-6	.0134	.116	69.0
2B-16	.0116	.108	69.5
2B-13	.0117	.108	66.0
2B-15	.0115	.107	69.5
2B-14	.0123	.111	65.0
Average		.111	66.6

TABLE XVIII

FATIGUE DATA, STEEL 3, 450°F TEMPER

Specimen No.	Rate ( $\alpha$ ), psi/cycle	Rate $1/2$ ( $\alpha$ ) $1/2$	Failure Stress, ksi
<u>High Rate</u>			
3-7	.152	.390	164
3-6	.115	.339	146
3-11	.156	.395	135.5
3-15	.156	.395	145
3-17	.156	.395	134
3-20	.157	.396	135
3-8	.156	.395	115
3-19	.155	.394	123
3-12	.153	.392	118
Average		.388	135.0
<u>Low Rate</u>			
3-18	.0119	.109	112
3-6	.0160	.108	117
3-7	.0165	.128	119
3-3	.0127	.113	111
3-13	.0120	.109	77
3-16	.0117	.108	78
3-5	.0138	.117	119
3-4	.0142	.119	102
3-10	.0145	.120	129.5
3-11	.0148	.122	141.5
Average		.115	110.6

TABLE XIX

FATIGUE DATA, STEEL 4, 500°F TEMPER

Specimen No.	Rate ( $\alpha$ ), psi/cycle	Rate $1/2$ ( $\alpha$ ) $1/2$	Failure Stress, ksi
<u>High Rate</u>			
4-4	.150	.387	175.5
4-14	.150	.387	108.5
4-3	.146	.382	165
4-6	.159	.398	131
4-12	.157	.397	171
4-17	.157	.397	123
Average		.391	145.7
<u>Low Rate</u>			
4-10	.0123	.111	142
4-9	.0158	.126	143
4-8	.0140	.118	125.5
4-7	.0137	.117	115
4-13	.0142	.119	167
4-19	.0148	.122	127
4-18	.0136	.117	127.5
Average		.119	135.3

TABLE XX

FATIGUE DATA, STEEL J, 475°F TEMPER

Specimen No.	Rate ( $\alpha$ ), psi/cycle	Rate $1/2$ ( $\alpha$ ) $1/2$	Failure Stress, ksi
<u>High Rate</u>			
J-8	.149	.386	125.5
J-17	.149	.386	127.5
J-13	.148	.385	153.5
J-4	.146	.382	137
J-9	.155	.394	136
J-15	.155	.394	146.5
J-3	.154	.392	115
J-5	.155	.394	141
J-12	.153	.391	137
Average		.389	135.4
<u>Low Rate</u>			
J-1	.0149	.122	118
J-14	.0146	.121	119
J-7	.0123	.111	118.5
J-16	.0152	.123	107
J-11	.0140	.118	124.5
J-6	.0122	.110	122
J-18	.0151	.123	133
J-10	.0143	.119	116.5
J-19	.0121	.110	128
J-2	.0159	.126	131
Average		.118	121.7

TABLE XXI

FATIGUE DATA, STEEL H, 500°F TEMPER

Specimen No.	Rate ( $\alpha$ ), psi/cycle	Rate $1/2$ ( $\alpha$ ) $1/2$	Failure Stress, ksi
<u>High Rate</u>			
H-18	.149	.386	154
H-1	.142	.377	138.5
H-5	.158	.397	145
H-7	.158	.397	141.5
H-10	.158	.397	120
H-14	.158	.397	129
H-13	.159	.399	130
H-2	.158	.397	145
Average		.393	137.8
<u>Low Rate</u>			
H-12	.0142	.119	103
H-8	.0147	.121	92
H-9	.0135	.116	105
H-17	.0148	.122	121
H-3	.0132	.115	115
H-11	.0148	.122	104
H-15	.0139	.118	129
H-16	.0142	.119	89
Average		.119	107.3

TABLE XXII

FATIGUE DATA, STEEL RVC, 475°F TEMPER

Specimen No.	Rate (a), psi/cycle	Rate 1/2 (a) 1/2	Failure Stress, ksi
<u>High Rate</u>			
RVC-16	.158	.397	143
RVC-3	.158	.397	151
RVC-9	.158	.397	146
RVC-11	.161	.401	148
RVC-6	.156	.394	151
RVC-15	.157	.396	151
RVC-10	.159	.399	155
Average		.397	149.3
<u>Low Rate</u>			
RVC-5	.0129	.113	104.5
RVC-13	.0136	.116	111
RVC-2	.0158	.125	124
RVC-7	.0137	.117	125
RVC-4	.0137	.117	136
RVC-8	.0129	.113	136
RVC-1	.0133	.115	122
RVC-17	.0132	.115	136
Average		.116	128.1

TABLE XXIII

FATIGUE DATA, STEEL DU, 550° + 600°F TEMPER

Specimen No.	Rate (a), psi/cycle	Rate $\frac{1}{2}$ (a) $\frac{1}{2}$	Failure Stress, ksi
<u>High Rate</u>			
DU-5	.147	.383	144
DU-7	.160	.400	156.5
DU-9	.160	.400	147.5
DU-6	.158	.397	151.5
DU-14	.158	.397	154
DU-16	.160	.400	155
DU-12	.161	.401	160
DU-15	.140	.374	160
Average		.394	153.5
<u>Low Rate</u>			
DU-11	.0164	.128	110
DU-4	.0136	.117	151
DU-13	.0142	.119	141.5
DU-8	.0160	.126	131
DU-1	.0160	.126	128.5
DU-3	.0160	.126	132.5
DU-10	.0153	.129	119
DU-17	.0143	.119	123.5
DU-2	.0143	.119	139
Average		.123	130.7

TABLE XXIV

FATIGUE DATA, STEEL DU NOTCHED, 550° + 600°F TEMPER

Specimen No.	Rate ( $\alpha$ ), psi/cycle	Rate $\frac{1}{2}$ ( $\alpha$ ) $\frac{1}{2}$	Failure Stress, ksi
<u>High Rate</u>			
DU-23	.162	.402	79
DU-29	.161	.401	82.5
DU-21	.163	.404	79
DU-33	.159	.399	83.5
DU-24	.150	.387	82
DU-31	.158	.397	82
DU-18	.158	.397	83
Average		.394	81.6
<u>Low Rate</u>			
DU-22	.0167	.129	70.5
DU-27	.0139	.118	65
DU-25	.0141	.119	72
DU-19	.0132	.115	67.5
DU-32	.0137	.118	68
DU-26	.0124	.111	68
DU-20	.0142	.119	68
DU-30	.0141	.119	71
Average		.119	68.8

FATIGUE DATA, STEEL D10B NOTCHED, 1050 °F TEMPER

Specimen No.	Rate (a), psi/cycle	Rate $1/2$ (a) $1/2$	Failure Stress, ksi
<u>High Rate</u>			
DB-2	.110	.332	81
DB-12	.138	.371	81.5
DB-11	.153	.391	78
DB-16	.150	.387	87
DB-3	.145	.381	85
DB-4	.148	.385	79
DB-17	.144	.379	78.5
DB-18	.146	.382	81
Average		.376	81.4
<u>Low Rate</u>			
DU-15	.0114	.107	74
DU-1	.0123	.111	76
DU-6	.0120	.109	66
DU-5	.0128	.113	68.5
DU-7	.0123	.111	71
DU-14	.0122	.110	71.5
DU-13	.0117	.108	68.5
DU-10	.0123	.111	72
DU-9	.0120	.109	68
DU-8	.0121	.111	73
DU-19	.0118	.109	68.5
Average		.110	70.6

TABLE XXVI

FATIGUE DATA, STEEL D10B NOTCHED, 1225°F TEMPER

Specimen No.	Rate ( $\alpha$ ), psi/cycle	Rate $1/2$ ( $\alpha$ ) $1/2$	Failure Stress, ksi
<u>High Rate</u>			
DB-40	.155	.394	77
DB-27	.153	.391	75.5
DB-38	.153	.391	75.5
DB-26	.145	.380	73
DB-34	.128	.357	74.5
DB-22	.148	.385	76
DB-23	.142	.377	78
DB-35	.135	.367	74
DB-25	.148	.385	76
DB-24	.145	.380	79
Average		.381	75.8
<u>Low Rate</u>			
DB-39	.0120	.109	67
DB-37	.0126	.112	57
DB-36	.0108	.104	58
DB-21	.0122	.110	62
DB-33	.0120	.109	64
DB-32	.0117	.108	67
DB-31	.0116	.108	67.5
DB-30	.0125	.112	65
DB-28	.0125	.112	63
Average		.109	63.4

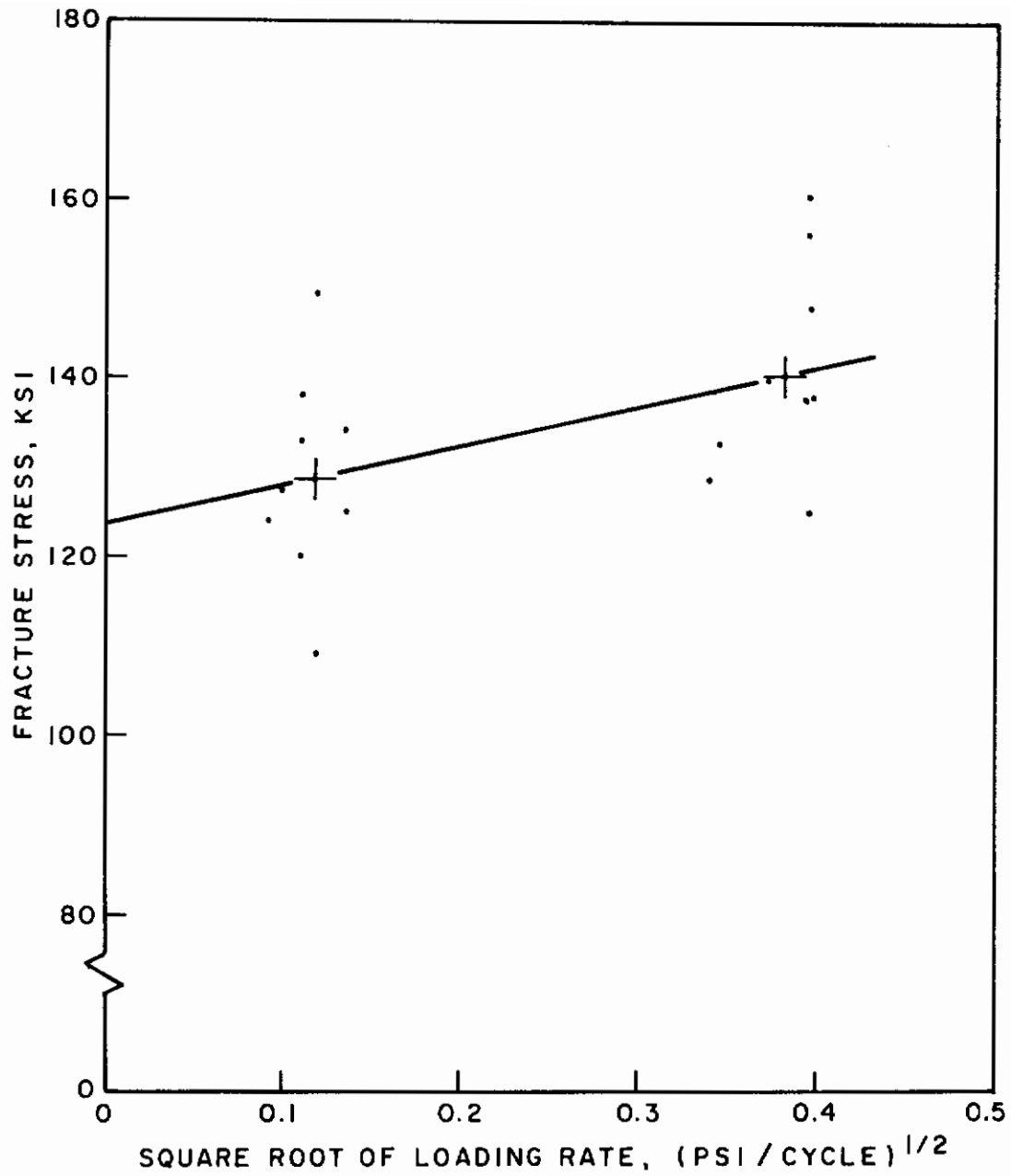


FIG.25 ROTATING BEAM PROT DIAGRAM.  
ALLOY I, 450° F TEMPER.

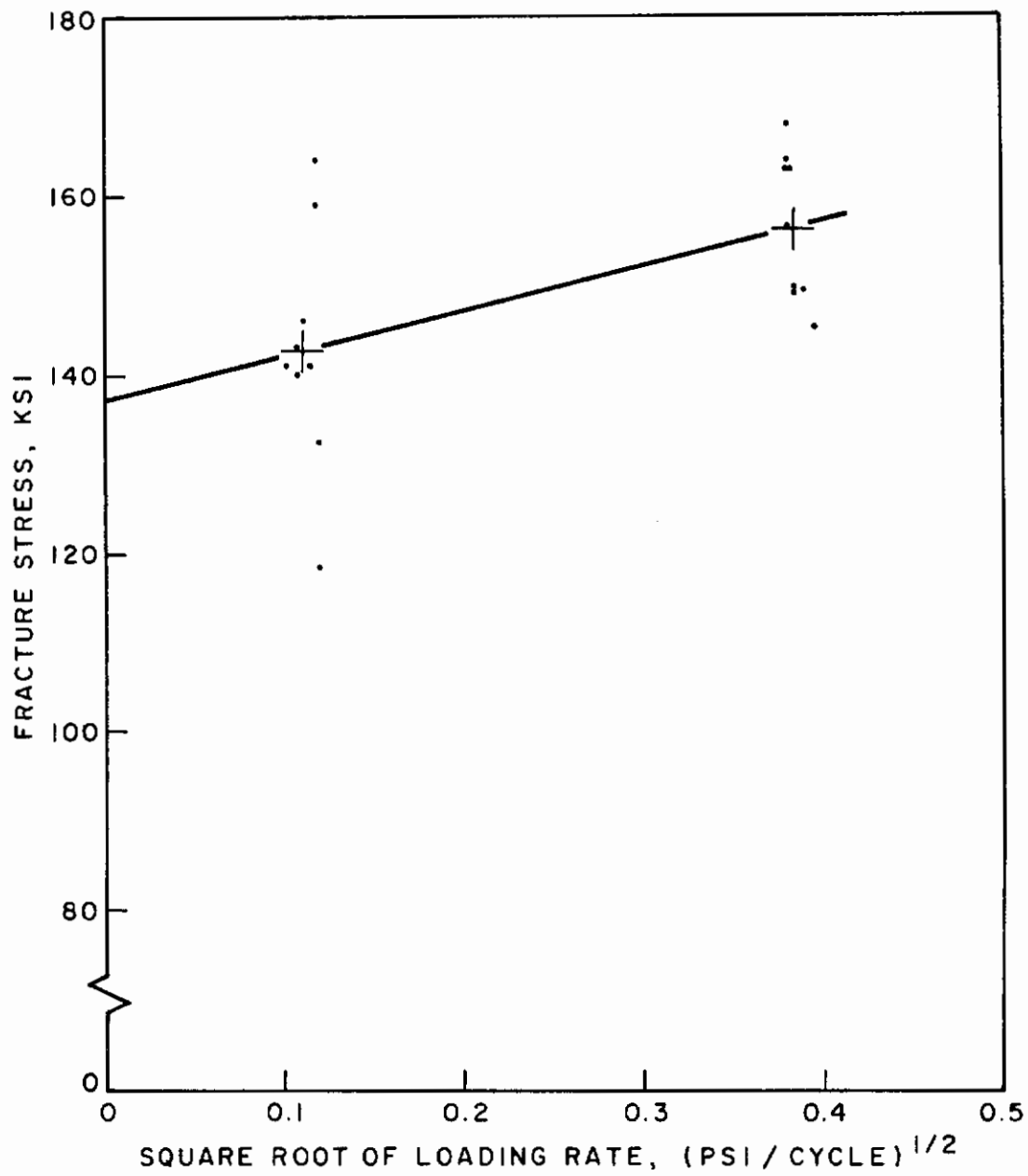


FIG.26 ROTATING BEAM PROT DIAGRAM  
ALLOY 2A, 450° F TEMPER.

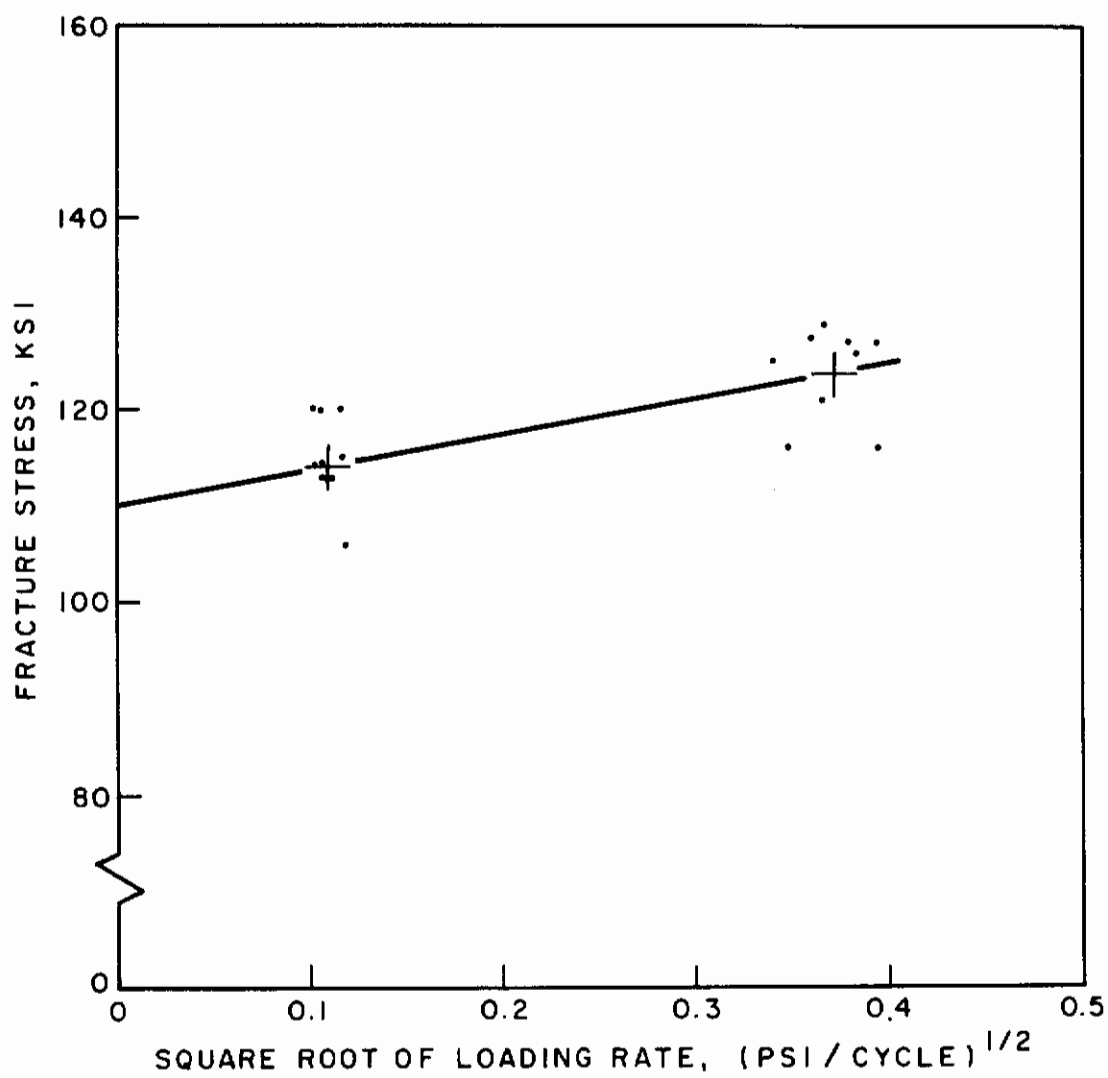


FIG.27 ROTATING BEAM PROT DIAGRAM.  
ALLOY 2A, 1000° F TEMPER.

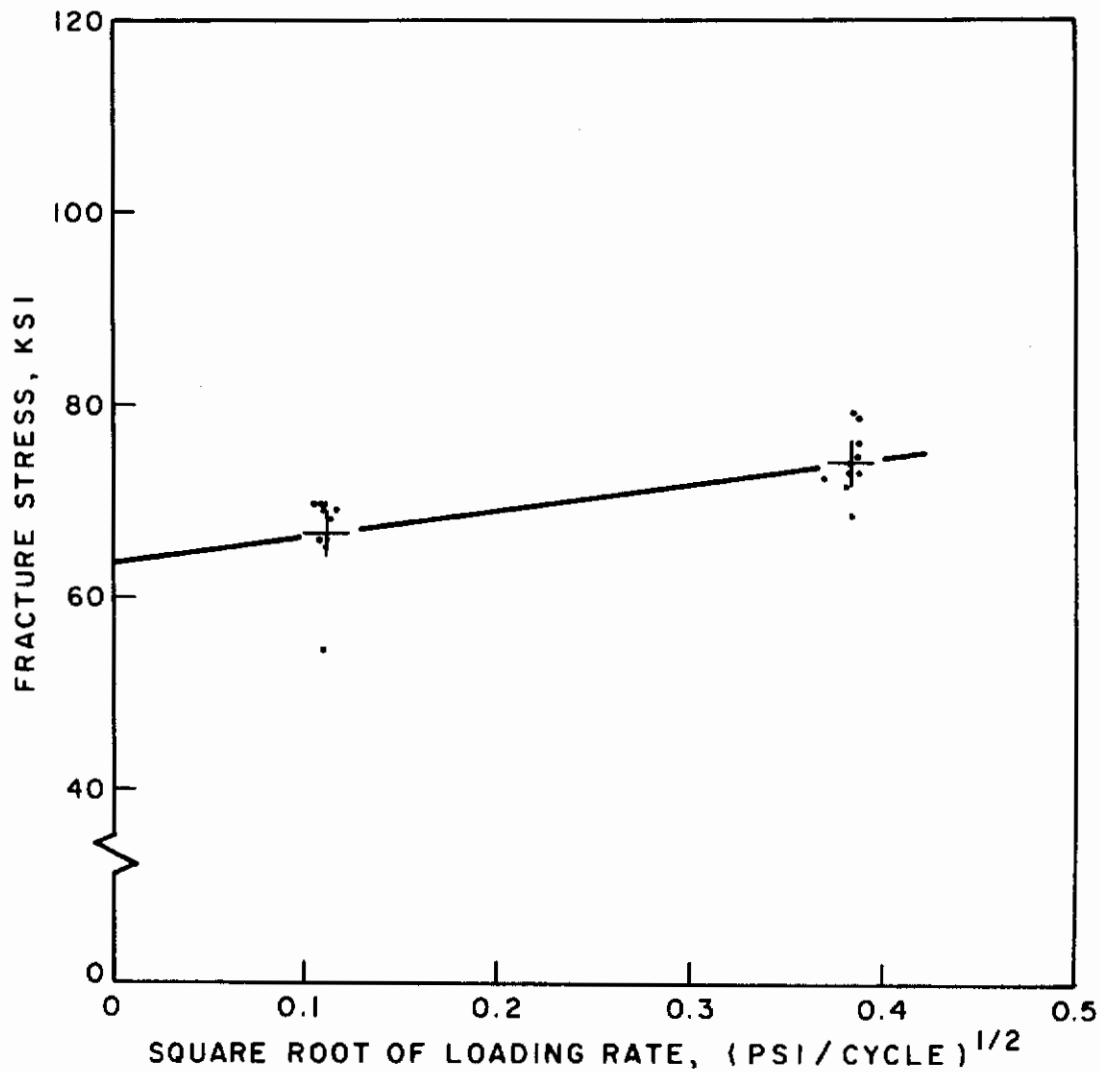


FIG.28 ROTATING BEAM PROT DIAGRAM.  
ALLOY 2B NOTCHED,  
475° F TEMPER.

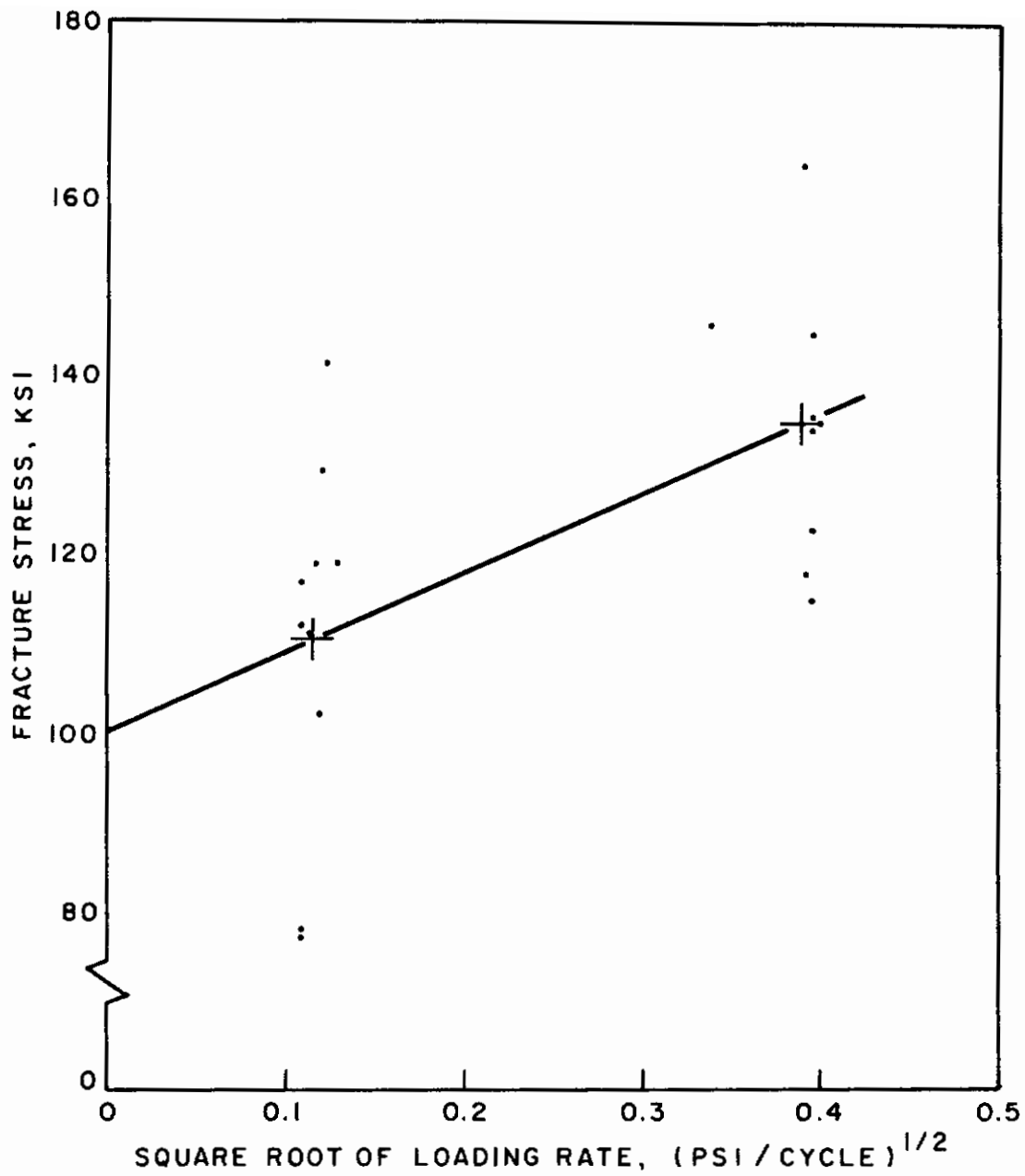


FIG.29 ROTATING BEAM PROT DIAGRAM.  
ALLOY 3, 450° F TEMPER.

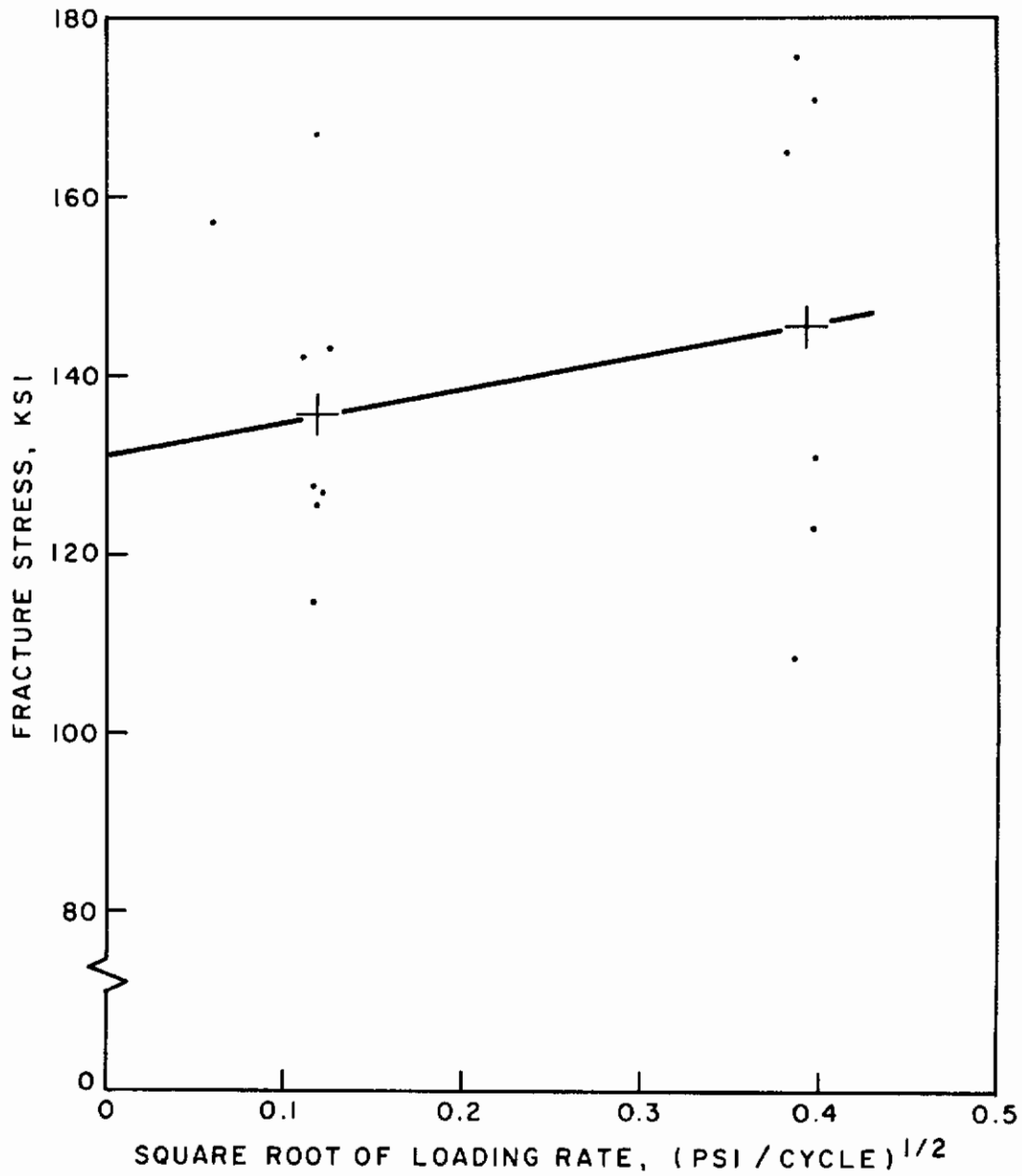


FIG.30 ROTATING BEAM PROT DIAGRAM.  
ALLOY 4, 500° F TEMPER.

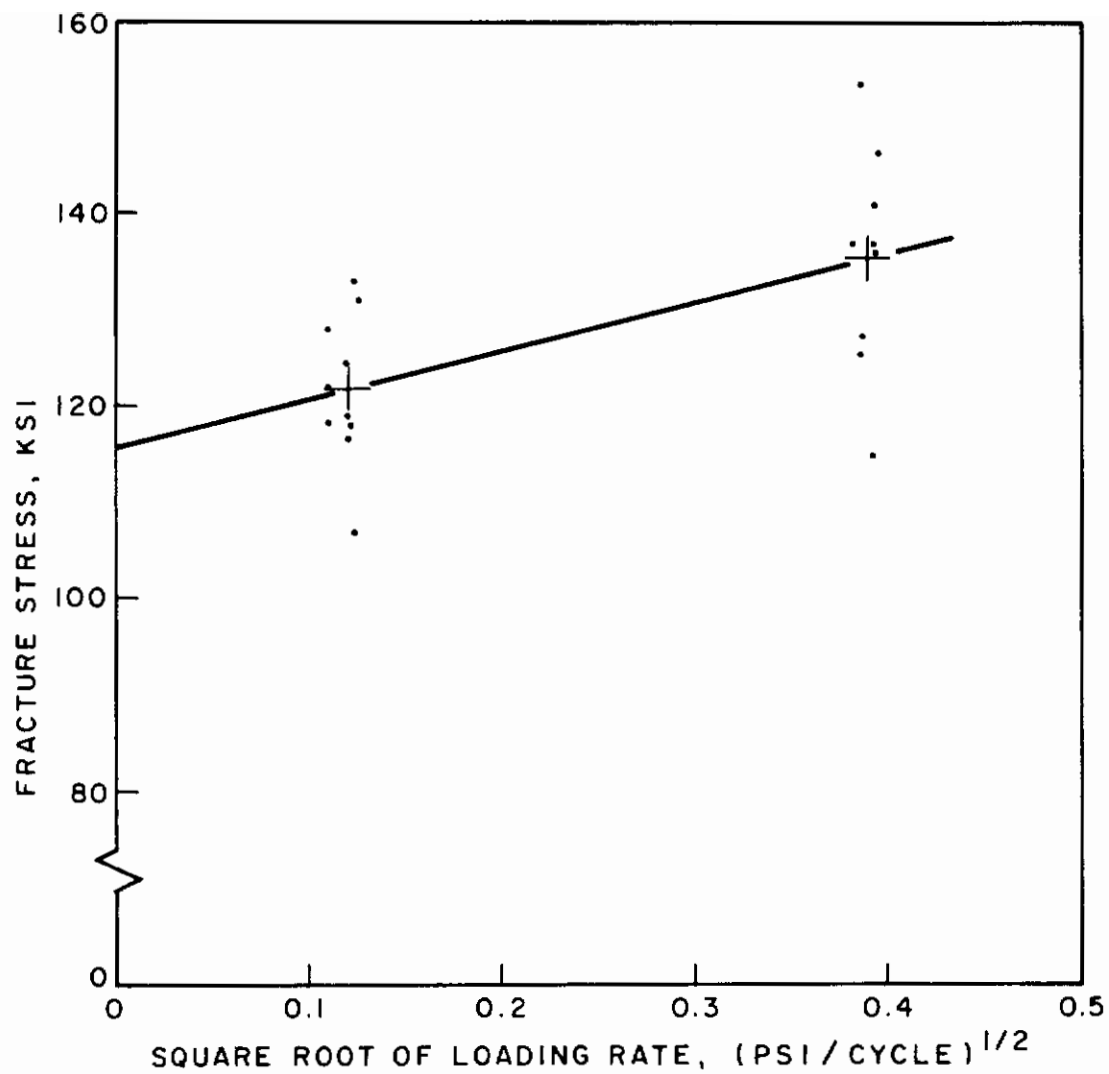


FIG.31 ROTATING BEAM PROT DIAGRAM.  
ALLOY J, 475° F TEMPER.

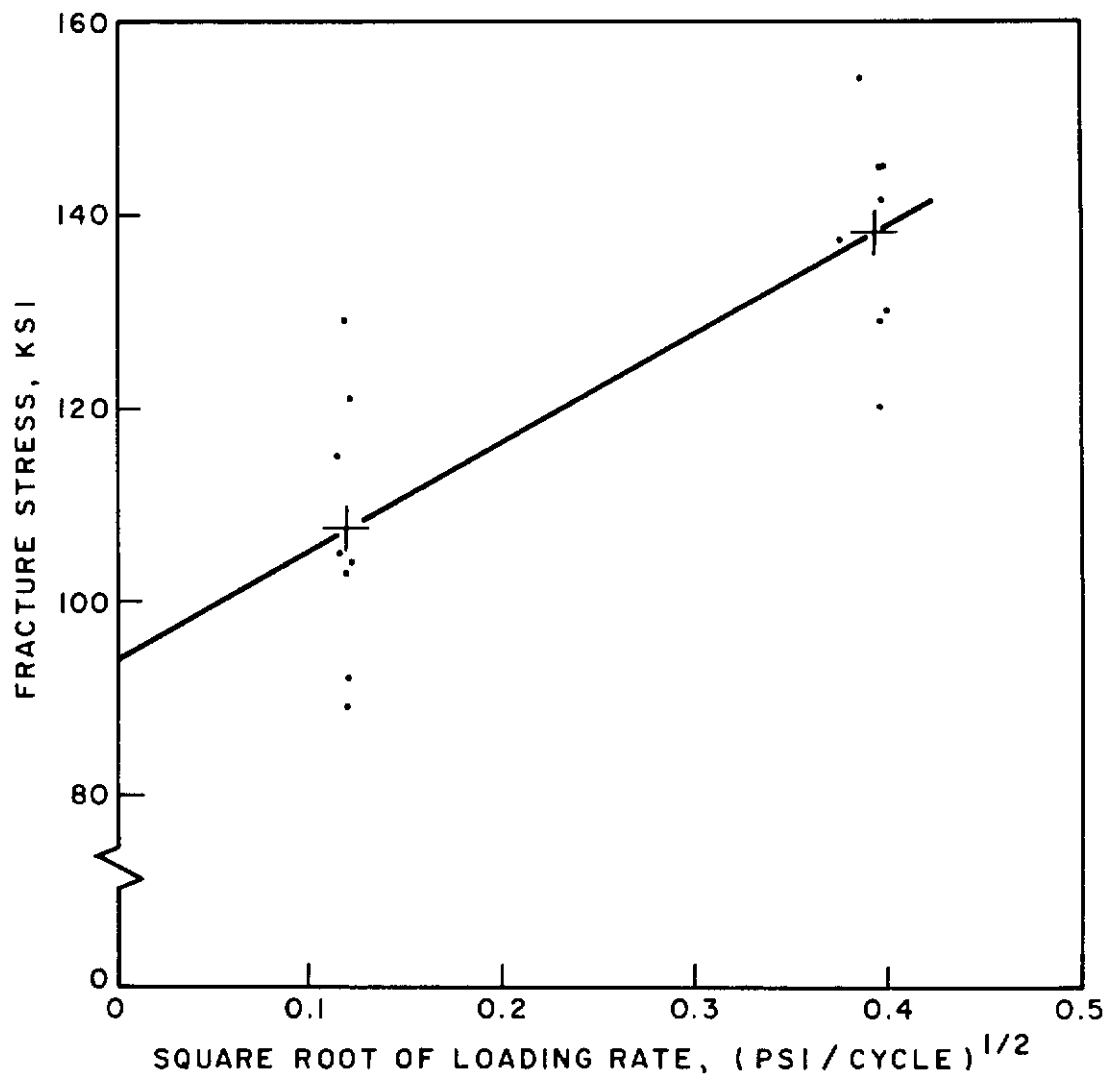


FIG.32 ROTATING BEAM PROT DIAGRAM.  
ALLOY H, 500°F TEMPER.

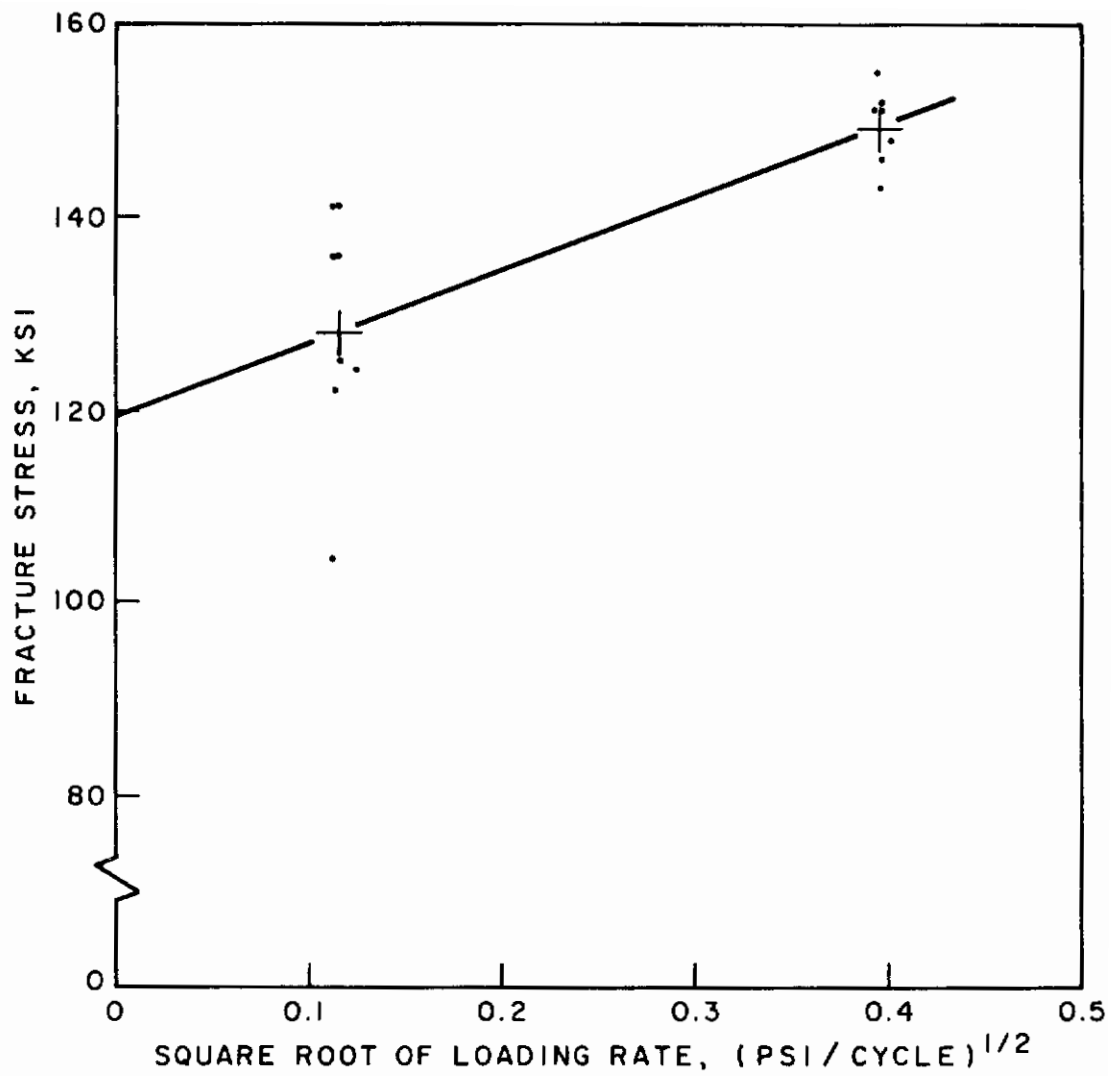


FIG.33 ROTATING BEAM PROT DIAGRAM.  
ALLOY RVC, 475°F TEMPER.

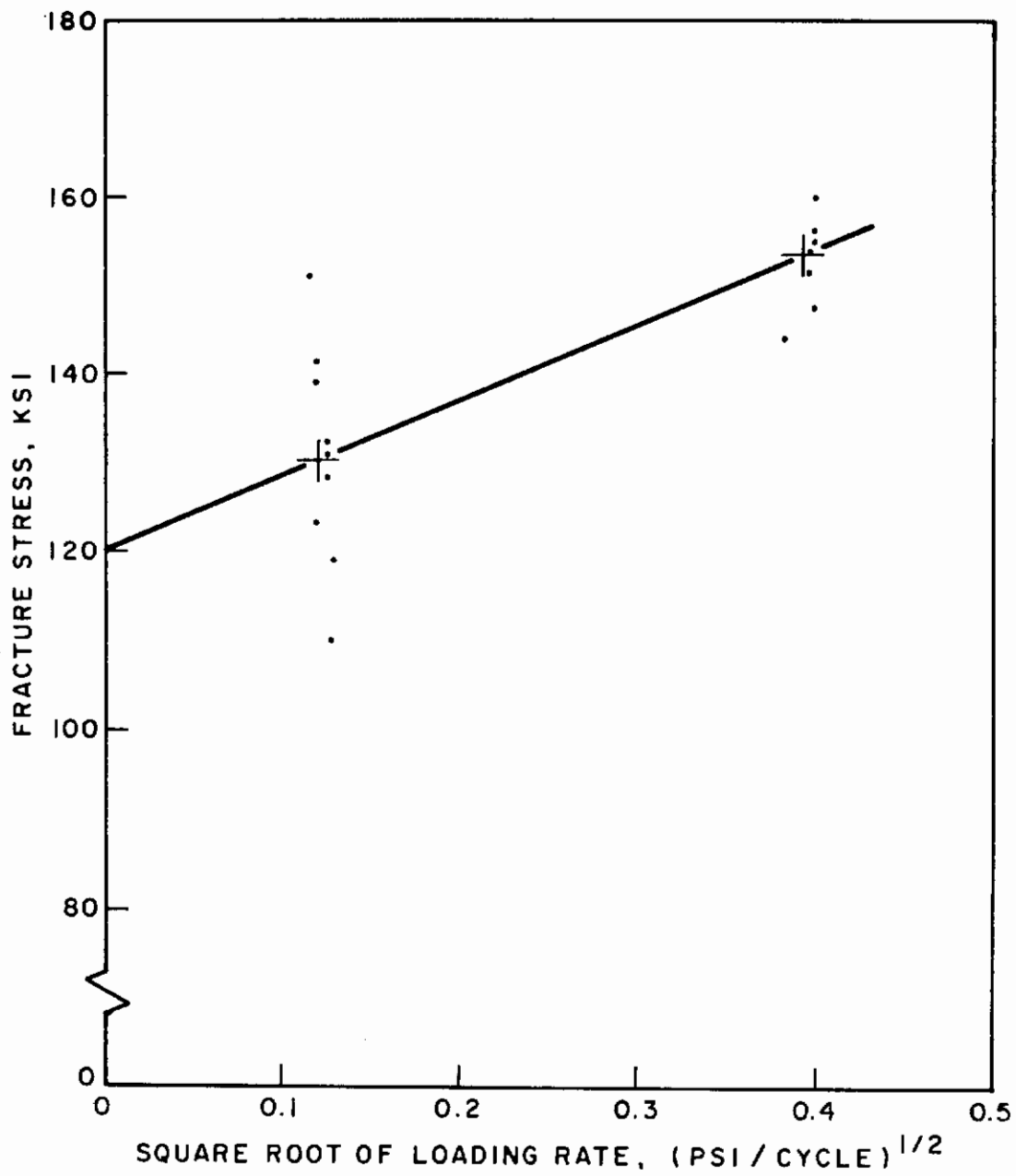


FIG. 34 ROTATING BEAM PROT DIAGRAM.  
ALLOY DU, 550° + 600° F TEMPER.

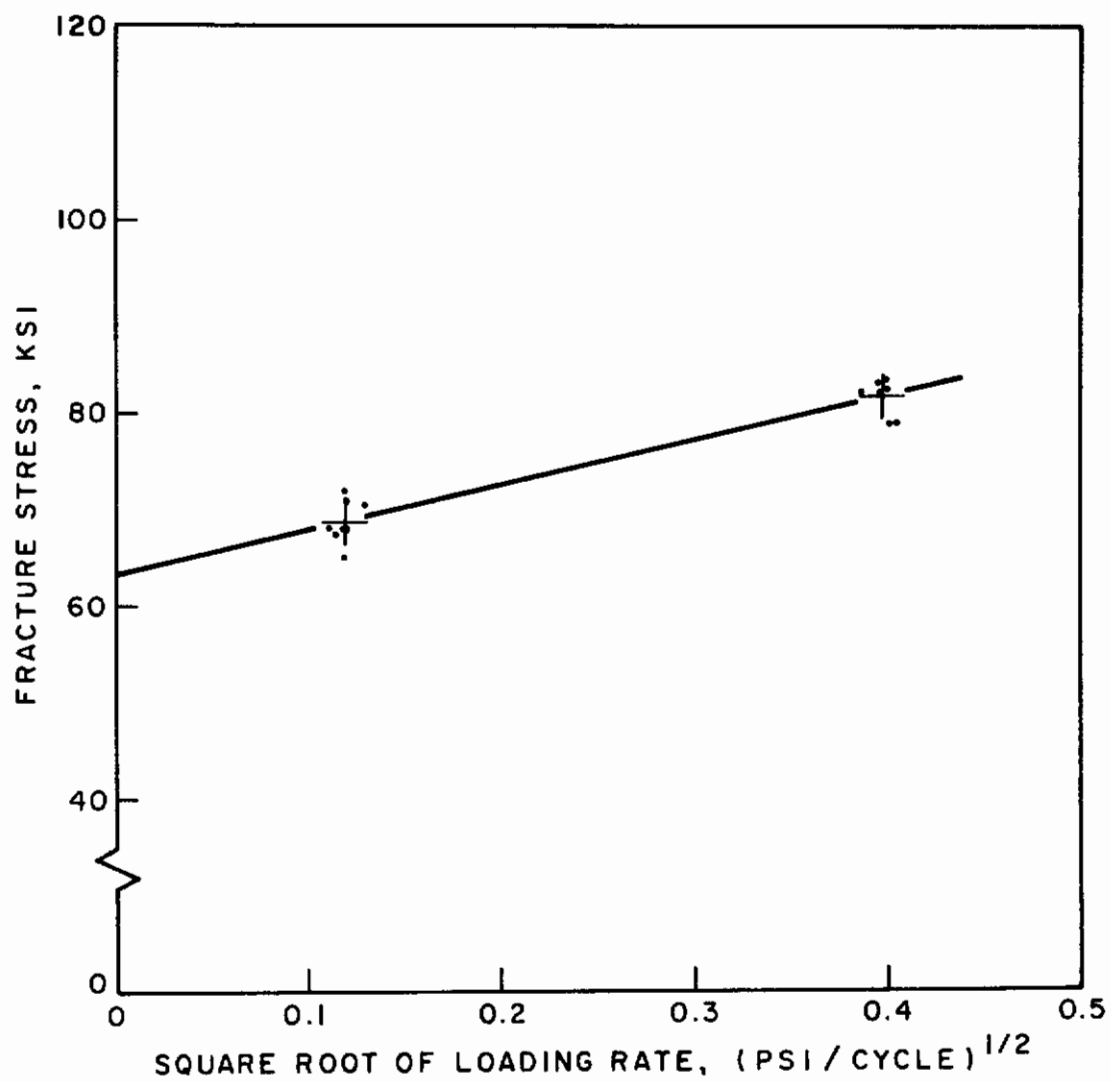


FIG.35 ROTATING BEAM PROT DIAGRAM.  
ALLOY DU NOTCHED,  
550° + 600° F TEMPER.

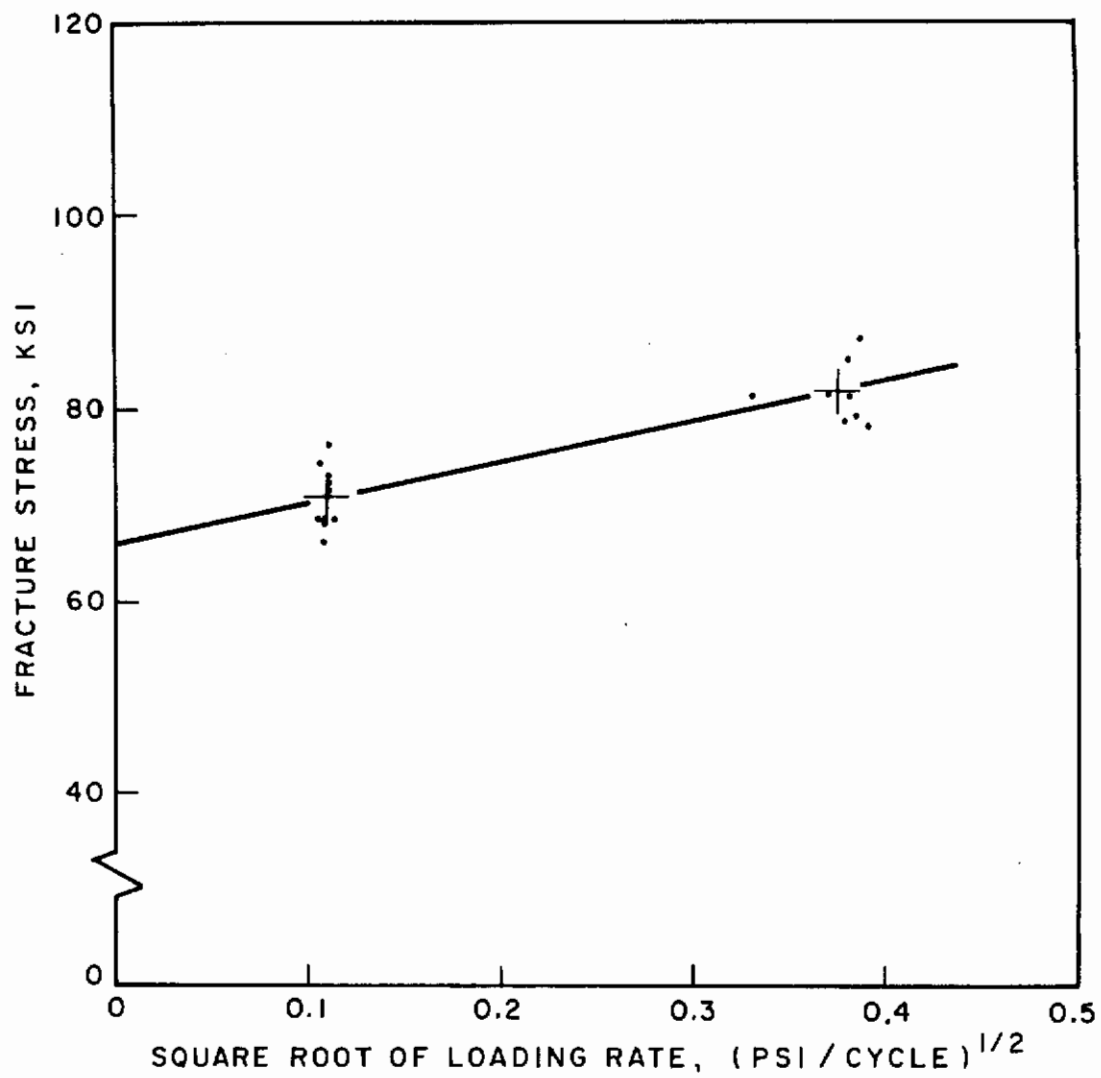


FIG.36 ROTATING BEAM PROT DIAGRAM.  
ALLOY DIOB NOTCHED,  
1050° F TEMPER.

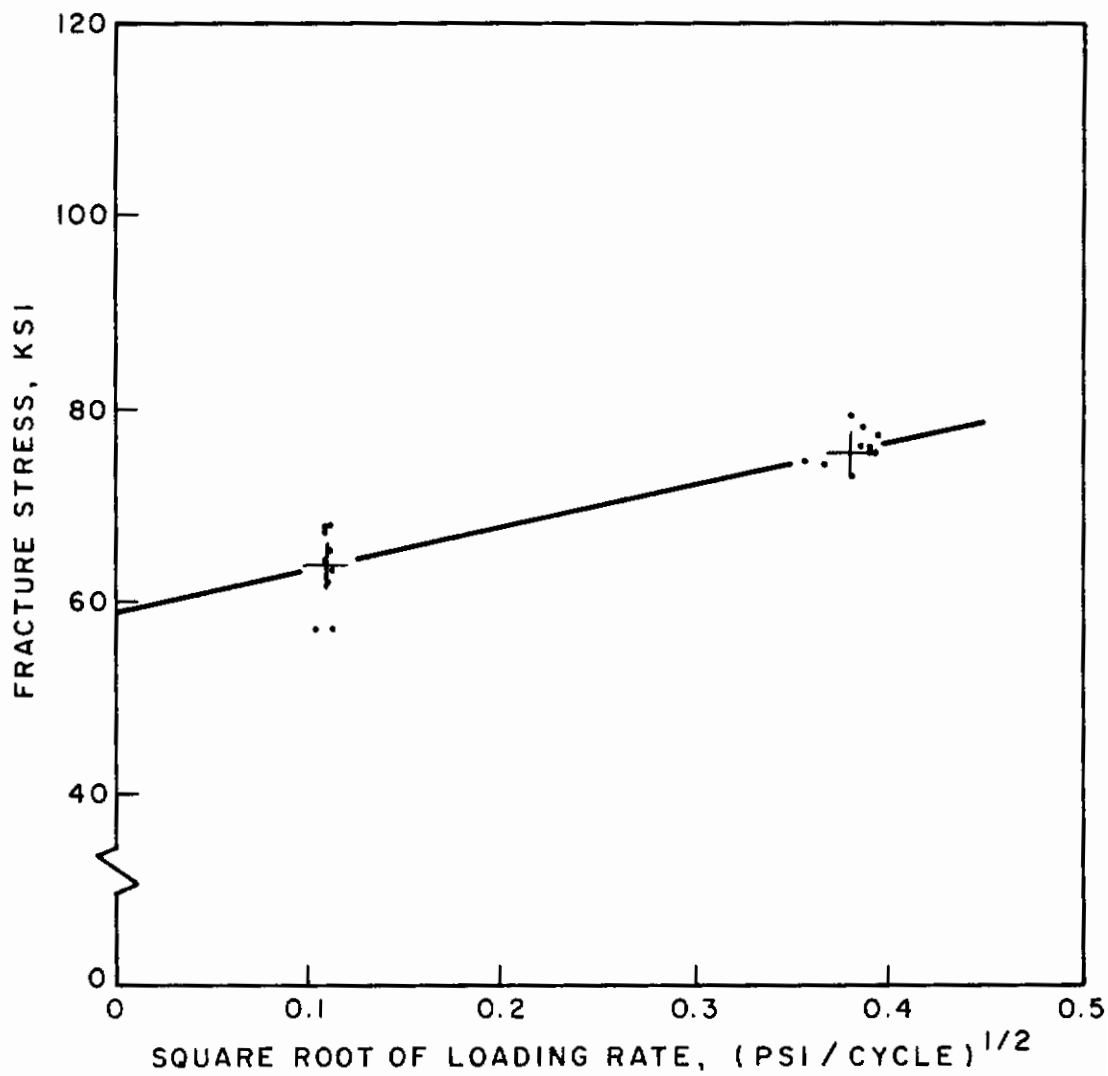


FIG. 37 ROTATING BEAM PROT DIAGRAM.  
ALLOY D10B NOTCHED,  
1225° F TEMPER,